

Dynamic Tests of High Strength Concrete Cylinders Considering Fiber Reinforcement and Elevated Temperature

A.M. Weidner
C.P. Pantelides
W. D. Richins
T. K. Larson
J. E. Blakeley

October 2012



The INL is a U.S. Department of Energy National Laboratory operated by Battelle Energy Alliance

DISCLAIMER

This information was prepared as an account of work sponsored by an agency of the U.S. Government. Neither the U.S. Government nor any agency thereof, nor any of their employees, makes any warranty, expressed or implied, or assumes any legal liability or responsibility for the accuracy, completeness, or usefulness, of any information, apparatus, product, or process disclosed, or represents that its use would not infringe privately owned rights. References herein to any specific commercial product, process, or service by trade name, trade mark, manufacturer, or otherwise, does not necessarily constitute or imply its endorsement, recommendation, or favoring by the U.S. Government or any agency thereof. The views and opinions of authors expressed herein do not necessarily state or reflect those of the U.S. Government or any agency thereof.

Drop Hammer Test on Concrete Cylinders Considering Fiber Reinforcement and Elevated Temperature

**A. M. Weidner
C. P. Pantelides
W. D. Richins
T. K. Larson
J. E. Blakeley**

October 2012

**Idaho National Laboratory
Idaho Falls, Idaho 83415**

<http://www.inl.gov>

**Prepared for the
U.S. Department of Energy
Through the INL LDRD Program
Under DOE Idaho Operations Office
Contract DE-AC07-05ID14517**

Abstract

Idaho National Laboratory engineers collaborated with students and staff from the University of Utah to perform a series of drop hammer impact tests of concrete cylinders. A facility, which allows for a hammer composed of steel weights to be dropped from a height of 16 ft, was built at the University of Utah Structures Laboratory to deliver the dynamic force. In July 2011 the drop hammer was used to perform tests on cylinders with and without fiber reinforcement from drop heights of 16 ft and 8 ft. In April 2012, additional tests were conducted using the same procedure on concrete cylinders at elevated temperatures. A data acquisition system was used to collect strain gauge and load cell data. The tests were also recorded using two high speed cameras. The tests were designed to determine the dynamic properties at high strain rates of normal weight concrete and fiber reinforced concrete in tension and compression at room and elevated temperatures.

Summary

Concrete, when loaded dynamically, has been reported to have a higher strength than when loaded statically. A variety of tests have been performed on different specimen types to determine dynamic impact factors (DIF) for concrete. The DIF is a ratio of the dynamic to static strength and is often reported as a function of the strain rate. Here, the DIF is taken as the ratio of the maximum dynamic to average static load. Several methods were developed to calculate the dynamic strain rate, the results of which were analyzed to determine which method was most accurate.

The DIF is of importance for defensive design purposes. The first phase of this project involved analyzing the performance of 4 ft. x 4 ft. concrete panels under blast loading¹. The results of these tests provided information about how different reinforcement types influence the performance of a structural member. To determine how the concrete material was influenced by dynamic loading at high strain rates, concrete cylinders were cast at the same time as the panels. The cylinders were 4 in. diameter by 8 in. high, and 6 in. diameter by 12 in. high. These cylinders were tested dynamically by dropping steel plates from elevated heights, using what is referred to as the drop hammer facility.

One form of reinforcement considered in the blast tests was fiber reinforced concrete (FRC), which is composed of macro-synthetic polypropylene fibers. One percent by volume of the FRC specimens consisted of 2 in. long Propex Concrete Systems Enduro 600 fibers. In July 2011, both FRC and normal weight concrete (NWC) cylinders were tested under different rates of dynamic impact by releasing a drop hammer weight from heights of 8 ft. and 16 ft.

When concrete is loaded dynamically in defense related facilities or nuclear power plants it is likely that it is also at an elevated temperature. In April 2012 additional tests were performed to determine how temperature, up to 400°F, affects the response of different concrete types under dynamic loading. These tests were of special interest in the case of fiber reinforced concrete. It is also possible that heated concrete can be loaded dynamically after it has had time to cool. A small number of tests were performed on cylinders that were allowed to cool down for approximately 18 hours after being heated to 400°F.

Tests were performed to determine both dynamic tension and compression properties at high strain rates for all specimen types. The dynamic test was designed and analyzed to follow standard static test procedures as close as possible so that a comparison between the two could be made. For this purpose, all types of dynamic tests were also performed statically.

For compression tests at room temperature, FRC specimens had higher DIFs and strain rates than NWC. However, for tension tests the DIF was lower for FRC specimens than for NWC specimens. At elevated temperatures, both compression and tension tests had lower DIFs and strain rates for FRC than NWC.

For the NWC compression tests, increasing the temperature increased the DIF and strain rate for 8 ft drop heights, but it decreased the DIF for 16 ft drop heights. For the NWC tension tests, increasing the temperature also caused a decrease in DIF and strain rate for the 16 ft drop height. All FRC specimens tested at elevated temperatures saw a decrease in DIF and strain rate when compared to room temperature results.

Acknowledgement

The authors acknowledge the assistance of Timothy Garfield, former University of Utah graduate student, for his work on the drop hammer facility and his involvement in the project and initial tests. The authors would also like to acknowledge Mark Bryant, University of Utah Structures Laboratory Technician, for his assistance in building and operating the drop hammer facility. The authors acknowledge the participation of the INL staff.

CONTENTS

Abstract.....	iv
Acknowledgement	v
Equipment and Data Collection	1
Drop Hammer Facility.....	1
High Speed Cameras	4
Strain Gauges.....	4
Load Cells.....	6
Satec™ Series Instron® Machine	8
Despatch Oven.....	9
Data Acquisition System	10
Figure 15 - Data Acquisition System.....	11
Test Setup and Procedure.....	12
July 2011 Dynamic Tests	12
April 2012 Dynamic Tests.....	12
Static Testing.....	15
July 2011 Dynamic Test Procedure.....	17
April 2012 Dynamic Test Procedure	18
Static Test Procedure.....	18
Data Reduction.....	21
DIAdem	21
Video Program.....	22
Partner™ Material Testing	22
Data Analysis.....	22
High Speed Camera Method.....	22
Load Cell Method.....	23
Strain Gauge Method.....	25
Results.....	30
Drop Height at Room Temperature	34
Drop Height at Elevated Temperature.....	38
Concrete Composition at Room Temperature	42
Concrete Composition at Elevated Temperature.....	42
Temperature Effects for Normal Weight Concrete	43
Temperature Effects for Fiber Reinforced Concrete	43
Conclusions.....	44

References.....	46
-----------------	----

FIGURES

Figure 1 - Drop Hammer Facility Model (Courtesy of Timothy Garfield1).....	2
Figure 2 - Drop Hammer Facility	3
Figure 3 - Drop Hammer.....	3
Figure 4 - Electrical Cable Hoist.....	3
Figure 5 - Time Lapse of Tension Tests	4
Figure 6 - Time Lapse of Compression Test.....	4
Figure 7 – Typical Strain Gauge Location and Cylinder Placement for Split Tension Tests	5
Figure 8 - Side Strain Gauge Location for Split Tension Tests	5
Figure 9 - Strain Gauge Location and Cylinder Placement for Compression Tests	6
Figure 10 - Load Cell System Assembly	7
Figure 11 - Load Cell System Configuration, July 2011	7
Figure 12 - Model 206C ICP Dynamic Force Sensor.....	7
Figure 13 - Hemispherical Steel Plate and Load Cell Configuration, April 2012	8
Figure 14 – Heating of Cylinders.....	9
Figure 15 - Data Acquisition System.....	11
Figure 16 – Specimen Placement for Dynamic Split Tension Tests.....	13
Figure 17 - Specimen Placement for Dynamic Compression Tests.....	13
Figure 18 - Static Compression Test.....	16
Figure 19 – Static Split Tension Test.....	16
Figure 20 - Drop Hammer Facility Set Up	20
Figure 21 – Despatch Oven.....	20
Figure 22 - Heated Cylinder	20
Figure 23 - Cylinder Transport	20
Figure 24 - Cylinder Placement	20
Figure 25 - Temperature Reading	21
Figure 26 - Data Acquisition System.....	21
Figure 27 - TF16 Load Data	24
Figure 28 - Area Considered for (a) Tension and (b) Compression.....	25
Figure 29 – TF16 Strain Data	26
Figure 30 - CF16 Strain Data.....	26

Figure 31 - CF16 Strain Data.....	26
Figure 32 - CN16 Strain Data.....	27
Figure 33 - CF8 Strain Data.....	27
Figure 34 – Comparison of Strain Rate Methods	30
Figure 35 - Dynamic Increase Factor vs. Strain Rate for July 2011	32
Figure 36 - Dynamic Increase Factor vs. Strain Rate for April 2012	32
Figure 37 – Malvar and Ross’s Comparison of Strain Rate Effects for Concrete in Tension7	33
Figure 38 – Millard, Molyneaux and Barnett’s Dynamic Increase Factor of Maximum Load with Strain8.....	33

TABLES

Table 1 - Data acquisition system details.....	11
Table 3 - July 2011 Dynamic Test Matrix	13
Table 4 - April 2012 Dynamic Test Matrix	14
Table 5 - Change in Drop Weights	14
Table 6 - July 2011 Static Test Matrix.....	17
Table 7 - April 2012 Static Test Matrix.....	17
Table 8 – Comparison of Strain Rate Methods for 8 ft Drop Height.....	28
Table 9 – Comparison of Strain Rate Methods for 16 ft Drop Height.....	29
Table 10 - July 2011, Static Test Results.....	35
Table 11 - July 2011, 8 ft Test Results	36
Table 12 - July 2011, 16 ft Test Results	37
Table 13 - April 2012, Static Test Results	39
Table 14 - April 2012, 8 ft Test Results.....	40
Table 15 - April 2012, 16 ft Test Results.....	41

Acronyms

DIF	Dynamic Increase Factor
ASTM	American Society for Testing and Materials
NWC	Normal Weight Concrete
FRC	Fiber Reinforce Concrete
TF	Tension, Fiber Reinforced Concrete, Static
CF	Compression, Fiber Reinforced Concrete, Static
TN	Tension, Normal Weight Concrete, Static
CN	Compression, Normal Weight Concrete, Static
TF8	Tension, Fiber Reinforced Concrete, 8 ft Drop Height
CF8	Compression, Fiber Reinforced Concrete, 8 ft Drop Height
TN8	Tension, Normal Weight Concrete, 8 ft Drop Height
CN8	Compression, Normal Weight Concrete, 8 ft Drop Height
TF16	Tension, Fiber Reinforced Concrete, 16 ft Drop Height
CF16	Compression, Fiber Reinforced Concrete, 16 ft Drop Height
TN16	Tension, Normal Weight Concrete, 16 ft Drop Height
CN16	Compression, Normal Weight Concrete, 16 ft Drop Height
TF0-400-4	Tension, Fiber Reinforced Concrete, Static, 400°F, 4 in. diameter cylinder
TF0-R-6	Tension, Fiber Reinforced Concrete, Static, Room Temperature, 6 in. diameter cylinder
CF0-400-4	Compression, Fiber Reinforced Concrete, Static, 400°F, 4 in. diameter cylinder
CF0-400-6	Compression, Fiber Reinforced Concrete, Static, 400°F, 6 in. diameter cylinder
CF0-R-6	Compression, Fiber Reinforced Concrete, Static, Room Temperature, 6 in. diameter cylinder
TN0-400-4	Tension, Normal Weight Concrete, Static, 400°F, 4 in. diameter cylinder
TN0-R-4	Tension, Normal Weight Concrete, Static, Room Temperature, 4 in. diameter cylinder
CN0-400-4	Compression, Normal Weight Concrete, Static, 400°F, 4 in. diameter cylinder
CN0-R-4	Compression, Normal Weight Concrete, Static, Room Temperature, 4 in. diameter cylinder

- TF8-400-4 Tension, Fiber Reinforced Concrete, 8 ft Drop Height, 400°F, 4 in. diameter cylinder
- CF8-400-4 Compression, Fiber Reinforced Concrete, 8 ft Drop Height, 400°F, 4 in. diameter cylinder
- TN8-400-4 Tension, Normal Weight Concrete, 8 ft Drop Height, 400°F, 4 in. diameter cylinder
- TN8-0-4 Tension, Normal Weight Concrete, 8 ft Drop Height, Room Temperature, 4 in. diameter cylinder
- CN8-400-4 Compression, Normal Weight Concrete, 8 ft Drop Height, 400°F, 4 in. diameter cylinder
- CN8-0-4 Compression, Normal Weight Concrete, 8 ft Drop Height, Room Temperature, 4 in. diameter cylinder
- TF16-400-4 Tension, Fiber Reinforced Concrete, 16 ft Drop Height, 400°F, 4 in. diameter cylinder
- CF16-400-4 Compression, Fiber Reinforced Concrete, 16 ft Drop Height, 400°F, 4 in. diameter cylinder
- TN16-400-4 Tension, Normal Weight Concrete, 16 ft Drop Height, 400°F, 4 in. diameter cylinder
- TN16-0-4 Tension, Normal Weight Concrete, 16 ft Drop Height, Room Temperature, 4 in. diameter cylinder
- CN16-400-4 Compression, Normal Weight Concrete, 16 ft Drop Height, 400°F, 4 in. diameter cylinder
- CN16-0-4 Compression, Normal Weight Concrete, 16 ft Drop Height, Room Temperature, 4 in. diameter cylinder
- CN16-cooled-4 Compression, Normal Weight Concrete, 16 ft Drop Height, Cooled for roughly 18 hours, 4 in. diameter cylinder

Equipment and Data Collection

A drop hammer facility at the University of Utah was built as part of this project and used to perform dynamic tests on concrete cylinders at high strain rates. High speed cameras, strain gauges and a load cell system were used to collect data during dynamic tests. Static tests were also performed using a Satec™ series Instron® machine. During one series of tests, cylinders were heated using a Despatch oven.

Drop Hammer Facility

To begin constructing the drop hammer facility a new foundation was cast to ensure that the dynamic force from the drop weight would have minimal effects on the surrounding facilities. The existing floor slab was replaced with a 7 ft by 9 ft by 4 ft deep concrete foundation. Gravel, 3 in. deep, was used as a base, and large pieces of steel were added as reinforcement. Twelve cubic feet of concrete was then cast and allowed to cure for 28 days to complete the foundation.

The base of the drop hammer structure is a 3 ft by 5 ft, 2 in. thick steel plate, as shown in Figure 1. Welded to the base plate are three, 23 ft tall legs made from 6 in. by 6 in. by 0.25 in. thick hollow steel square tubes. The main section of the drop hammer is a 0.25 in. thick, 16 in. diameter pipe, through the drop weight falls.

The legs and tube are connected by welded and bolted plates along the length of the drop hammer. The pipe is slotted in the front to help prevent the drop weight from binding in the tube. One foot increment markings, measured from the impact target where the cylinder is placed, are shown on the side of the slotted pipe. To complete the facility, a protective cage was built around the base of the drop hammer to reduce the spread of concrete as the specimens break. An image of the finished drop hammer is shown in Figure 2.

The drop weight used to deliver the dynamic load is composed of 14 in. diameter steel plates with a thickness of either 0.5 or 1 in. These plates, have a central hole diameter of 1.25 in. and were added to a 1 in. thick base plate with a 1 in. diameter rod welded through its center.

Once the desired drop weight was reached, a square tube was placed on the base plate rod. The square tube had a checker board pattern placed on it to calculate the velocity of the drop hammer as it fell using high speed camera recordings. An additional thin plate was then placed on top of the square tube. To finalize the drop hammer, the plates and square tube were tightened together using a fastening gig which was bolted onto the base plate rod. This configuration, shown in Figure 3, was designed to distribute the weight along the length of the drop hammer, thus preventing it from oscillating as it fell. The drop hammer was connected to an electric cable hoist using a quick release hook as shown in Figure 4.

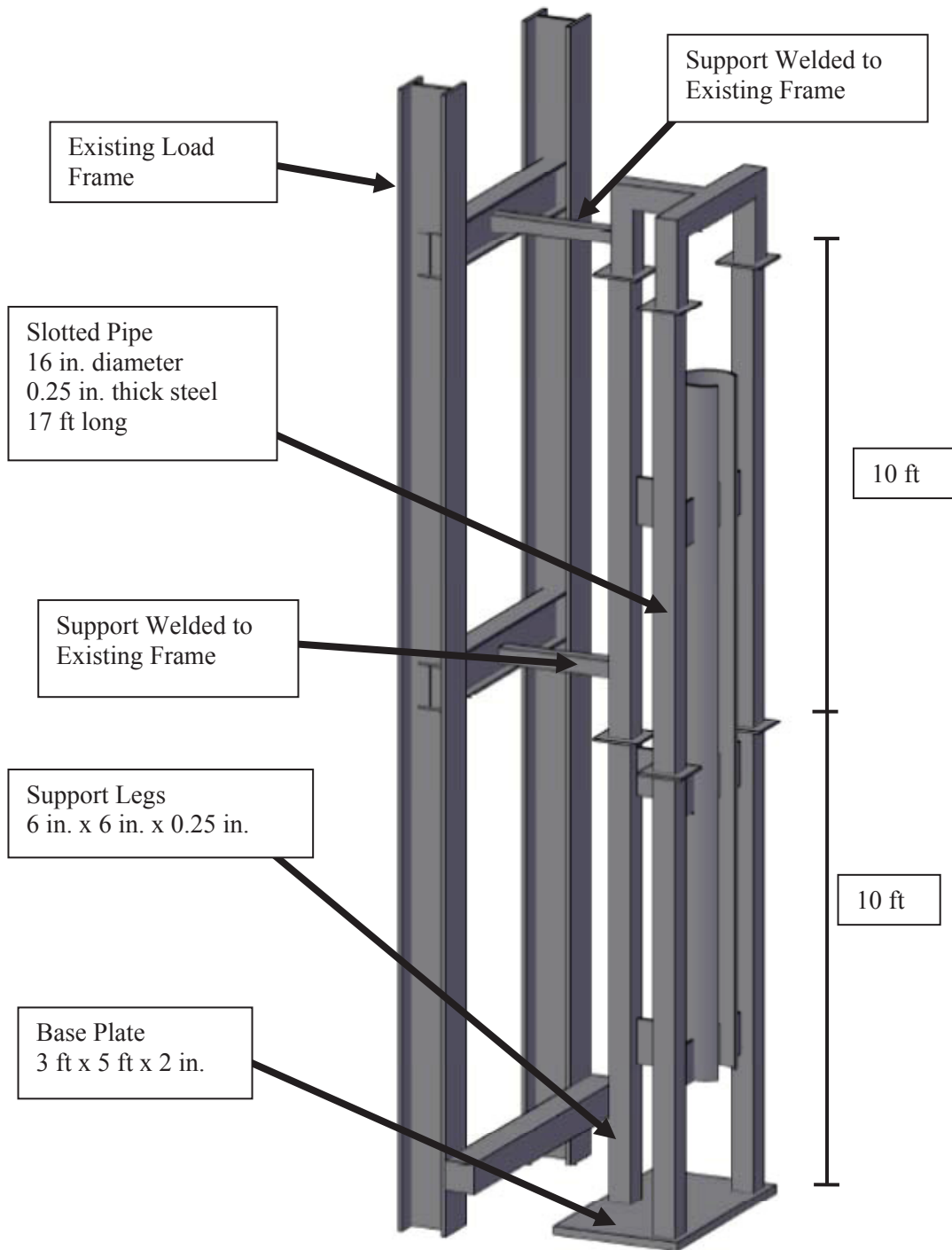


Figure 1 - Drop Hammer Facility Model (Courtesy of Timothy Garfield¹)

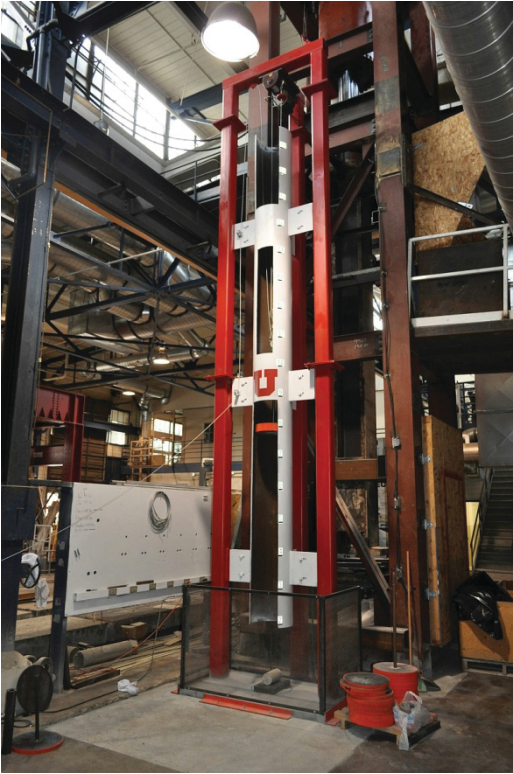


Figure 2 - Drop Hammer Facility



Figure 4 - Electrical Cable Hoist

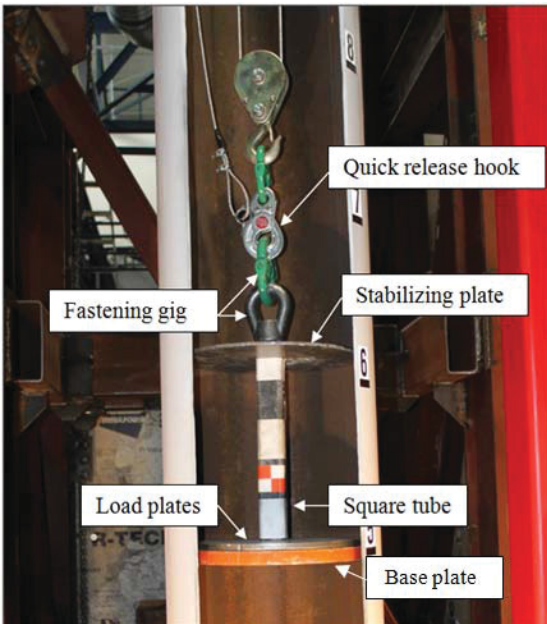


Figure 3 - Drop Hammer

High Speed Cameras

During the July 2011 tests, two high speed cameras were used to record failure of the specimens. A Phantom v12 camera with a signal to noise ratio of 7968, an exposure of 99 microseconds and a resolution of 400x504 pixels was placed directly in front of the specimen and recorded the tests at a rate of 8000 frames per second (FPS). A second camera, a Phantom v7.3 with a signal to noise ratio of 7966, an exposure of 123 microseconds and a resolution of 640x480 pixels, was placed toward the side of the specimen, recording at a rate of 7005 FPS.

To achieve high quality videos, shop lights were required during tests. A touch pad was used to signal the cameras to begin recording. The touch pad was triggered as the hammer was being released. To demonstrate the data recorded, consecutive image shots of the video are shown in Figure 5 for tension and Figure 6 for compression.

Strain Gauges

For the July 2011 tests, 120 ohms strain gauges were placed on each specimen. Micro-Measurements (Vishay) strain gauges were used. Most specimens had two strain gauges: the first was a model 10CBE, 1 in. gauge (referred to as Strain Gauge 0) and the second a model 20CBW, 2 in. gauge (referred to as Strain Gauge 1). For the splitting tension tests, two strain gauges were placed on

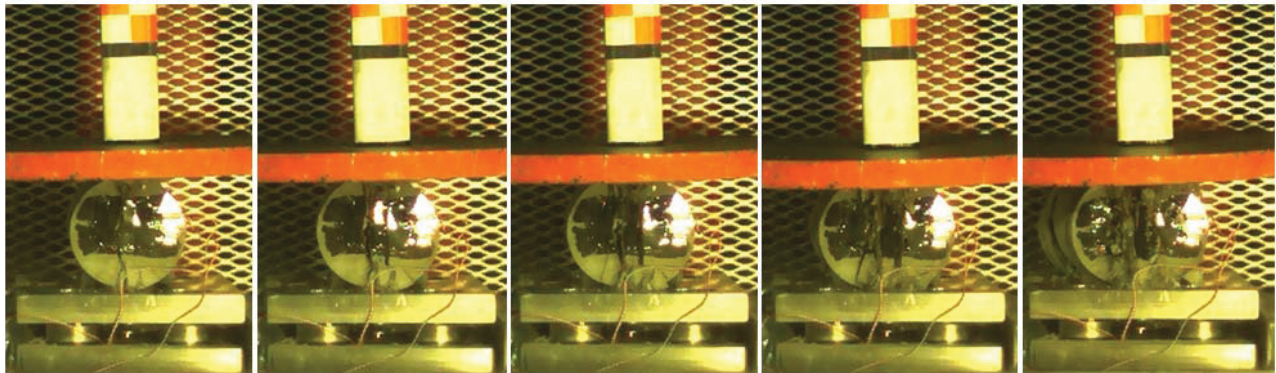


Figure 5 - Time Lapse of Tension Tests

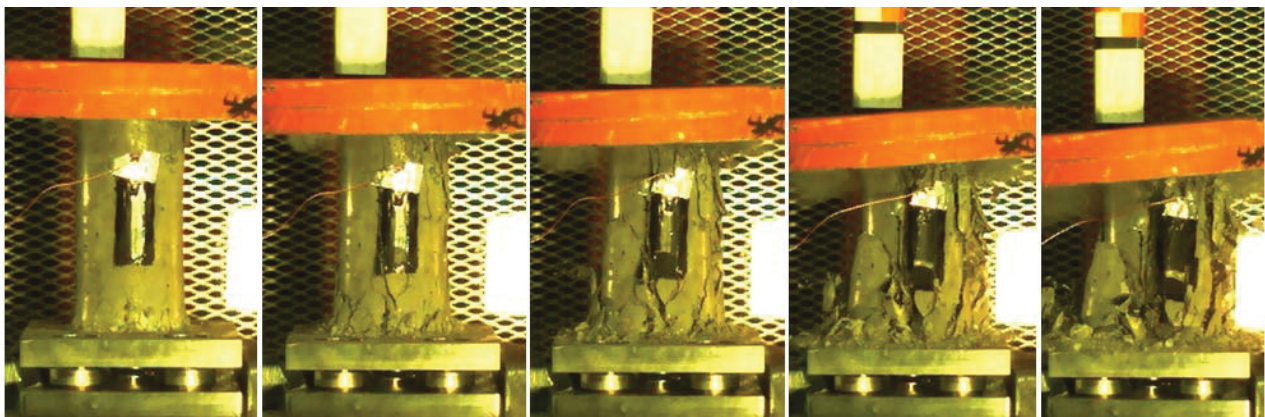


Figure 6 - Time Lapse of Compression Test

the top face of the cylinder and the drop weight was released onto the side of the cylinder, as shown in Figure 7. This configuration was typical for most tests; however, some splitting tension specimens had gauges on their sides instead of the top face (Figure 8) due to a limitation of appropriate strain gauge configuration. For the compression tests, two strain gauges were placed on opposite vertical sides and the drop weight was released onto the top face of the cylinder as shown in Figure 9. There were a number of instances where one of the strain gauges failed and no output was recorded.

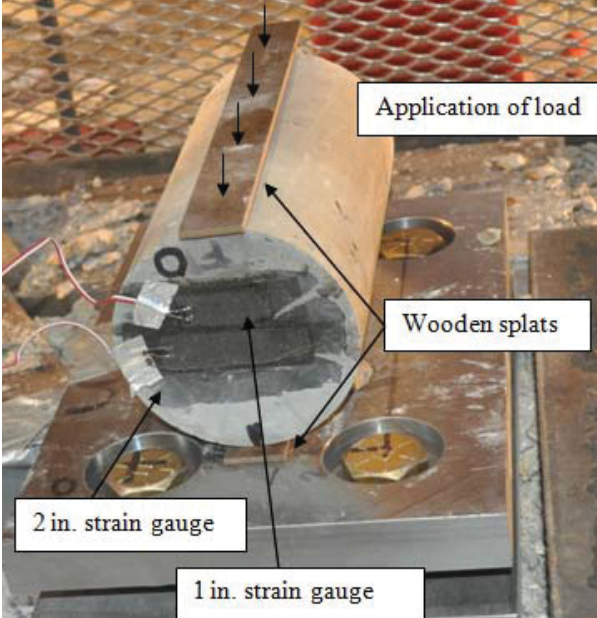


Figure 7 – Typical Strain Gauge Location and Cylinder Placement for Split Tension Tests

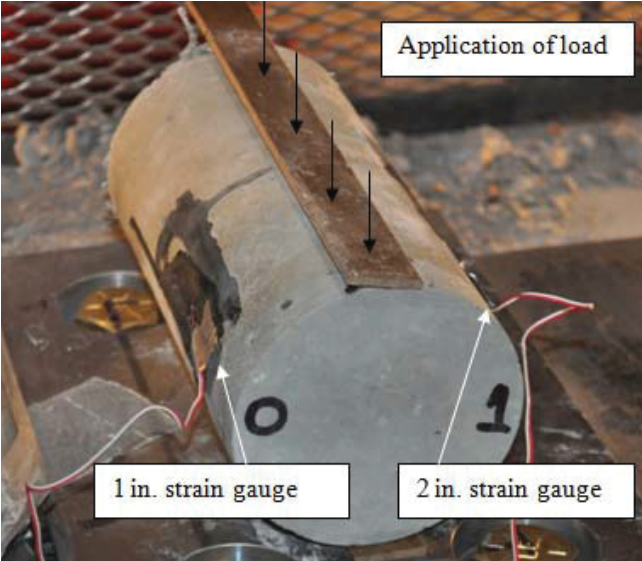


Figure 8 - Side Strain Gauge Location for Split Tension Tests

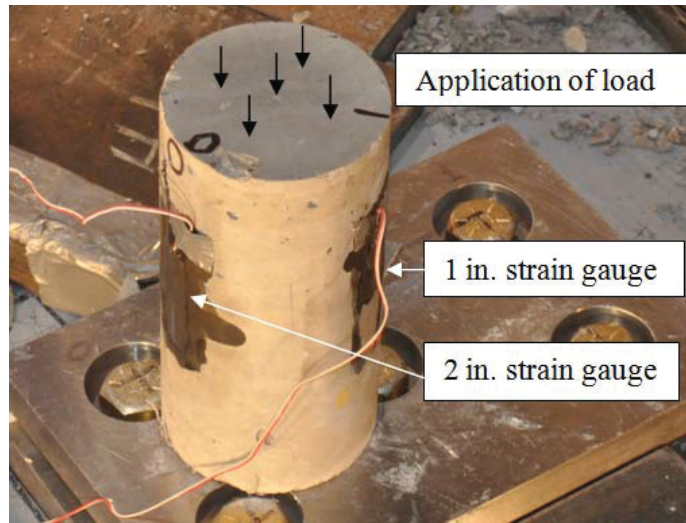


Figure 9 - Strain Gauge Location and Cylinder Placement for Compression Tests

Load Cells

To measure the dynamic load on the cylinders, a load cell system composed of dynamic force sensors, steel plates, and mounting hardware, was built. For the load cell sensors to record accurate data, they need to be loaded concentrically to reduce the possibility of induced bending moments. This is best achieved by using multiple sensors placed between two flat plates that prevent the sensor from bending.

Five force sensors were placed between two, 12 in. by 8 in. by 1 in. thick steel plates. The load sensors and plates were held together using HEX HD 7/8-14 UNF-2B x 1-3/4 LG bolts. These bolts are elastic, which allows for the applied force to transfer to the force sensor. Two anti-friction washers, placed above and below each sensor, are used to protect the surface of the sensor when the mounting bolt is being tightened. A schematic of the load cell system assembly is shown in Figure 10. The final load cell system is shown in Figure 11.

Model 206C ICP® Dynamic Force Sensors (Figure 12), which can record up to 80,000 pounds of force, were used in the load cell system. A constant current between 2 and 20 mA was supplied to the sensor from the data acquisition system. When a load was applied, the sensor measured the high impedance of the supplied current and converted it to a low impedance voltage signal that was recorded. The sensors had a target pre-load of 16,000 pounds, which is required to ensure that the sensor will perform as calibrated².

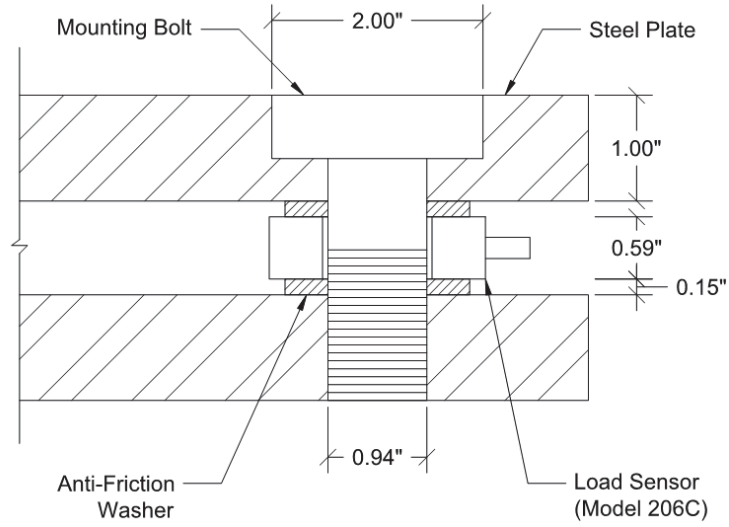


Figure 10 - Load Cell System Assembly



Figure 11 - Load Cell System Configuration, July 2011



Figure 12 - Model 206C ICP Dynamic Force Sensor

To achieve this pre-load amount the initial pre-load and voltage was measured using the data acquisition system and a digital voltmeter respectively. A ratio of the current pre-load to the target pre-load was added to the measured voltage. This calculated value was the desired voltage. A torque was applied to the mounting studs until the desired voltage was achieved, as measured from the digital voltmeter. If necessary, as determined from analyzing the output of the sensors after tests, the load cells were readjusted back to the proper pre-load value.

For the July 2011 tests the load cell system was held in place on the drop hammer facility's base plate by placing steel plates around it. In April 2012, small steel angles were welded to the drop hammer facility's base plate to hold the load cell system in place. In addition, a hemispherical steel plate was placed on top of the load cell system during tests.

As shown in Figure 13, the hemispherical plate is composed of two joining convex and concave hemispherical plates. Reviewing the individual load cell data from the July 2011 tests showed that some force sensors were recording significantly larger loads than others. It was believed that the plate containing the load cells was deflecting unevenly during tests due to concentrated forces. The hemispherical plate was added to the testing configuration to distribute the load more evenly among the load cells, and to prevent the load cell system plates from deflecting unevenly.

Satec™ Series Instron® Machine

A Satec™ Series Instron® machine was used to test the concrete cylinders statically. The Instron machine applied a constantly increasing load to the cylinders. The American Society for Testing and Materials (ASTM) standard C496/C496M-04e1 Standard Test Method for Splitting Strength of Cylindrical Concrete Specimens³ and C39/C39M-09a Standard Test Method for Compressive Strength of Cylindrical Concrete⁴ were used to determine the appropriate loading rate. The loading rate is a function of the size of cylinder used. Equations (1) and (2) were used to determine the loading rate for split tension and compression respectively.

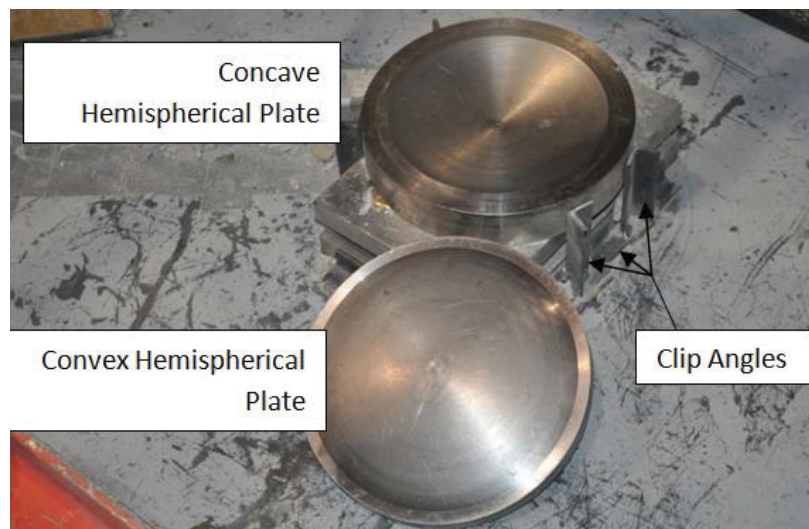


Figure 13 - Hemispherical Steel Plate and Load Cell Configuration, April 2012

$$Tension\ Applied\ Loading\ Rate = 2.5\ psi/sec * \frac{\pi * L * D}{2} \quad (1)$$

$$Compression\ Applied\ Loading\ Rate = 40\ psi/sec * \frac{\pi * D^2}{4} \quad (2)$$

For the 4 in. diameter by 8 in. long cylinders, the loading rates were 500 pound force per sec (lbf/sec) and 130 lbf/sec for compression and tension respectively. For 6 in. diameter by 12 in. long cylinders, the loading rate was 1130 lbf/sec and 285 lbf/sec for compression and tension respectively.

Despatch Oven

An LBB2-18-1 Despatch oven, with a maximum temperature of 400°F was used to heat the cylinders for the April 2012 tests. To determine the time required for the cylinder to be placed in the oven, a thermocouple was placed on a NWC 4 in. diameter by 8 in. high cylinder and a NWC 6 in. diameter by 12 in. high cylinder. The resulting rate of temperature increase is shown in Figure 14. The maximum interior temperature reached for the 4 in. diameter by 8 in. high cylinders was 386°F. For the 6 in. diameter by 12 in. high cylinders, the maximum temperature was 381°F. The 4 in. diameter by 8 in. high cylinder reached its maximum temperature after approximately 5 hours. The 6 in. diameter by 12 in. high cylinder took significantly longer to reach its maximum temperature. From these results, it was decided to allow all cylinders 24 hours of heating before being tested.

Specimen types CN0-400, CN8-400, CN16-400 and TN16-400-1, comprising 15 cylinders, were placed in the oven when it was not preheated. Twenty one additional cylinders, specimen types TN16-400, TN8-400 and CN16-cooled, were added 31 hours later. At 52 hours of heating, specimen types TF16-400, CF16-400 and CF8-400 were added to the oven. At this point in time several of the heated cylinders had been removed and tested but many cylinders still remained in the oven. Two hours later, TF8-400, CF0-400, TN0-400 and TF0-400 were also added to the oven. At this point in time many of the fully heated cylinders had been removed.

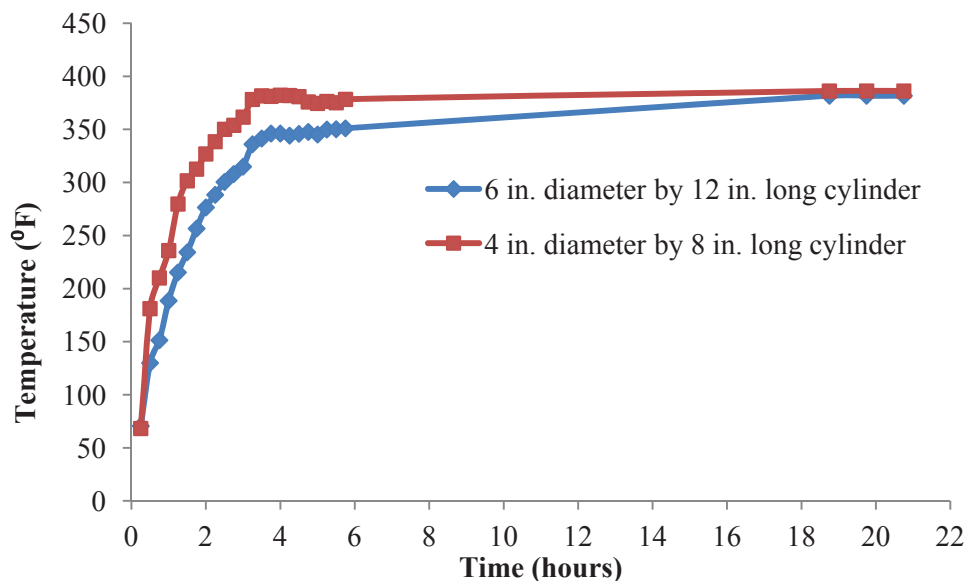


Figure 14 – Heating of Cylinders

The addition of so many room temperature specimens caused the surface temperature of the remaining fully heated cylinders to decrease. The interior temperature of the cylinder was most likely maintained during the addition of the room temperature cylinders. However, since the recorded temperature value was that of the surface temperature, testing was delayed until the surface temperature of all cylinders once again reached the typical maximum readings. This would result in recorded temperatures that were more reflective of the interior temperature of the cylinder. The approximate amount of time each specimen was placed in the oven is shown in Table 2.

The surface temperature of the cylinders was measured using a Fluke® 65 infrared thermometer. Temperatures were recorded as the cylinders came out of the oven and just prior to testing. The temperatures of the cylinders as they were coming out of the oven ranged from 352°F to 407°F, with an average temperature of 391°F. Readings between 323°F and 365°F, with an average of 353°F, were recorded just prior to testing. By comparison, the room temperature cylinders had an average surface temperature of 63°F.

Data Acquisition System

The data acquisition system consisted of National Instruments PXI hardware installed in a portable Hardigg case shown in Figure 15. Power and signal conditioning for the PCB force sensors were provided by a PCB Model 481A02 16-channel signal conditioner. Force sensor data were recorded for 6 seconds at 1×10^5 samples/second. Data for the strain gauges were recorded at 2×10^4 samples/sec. Details of the instrumentation are shown in Table 1.

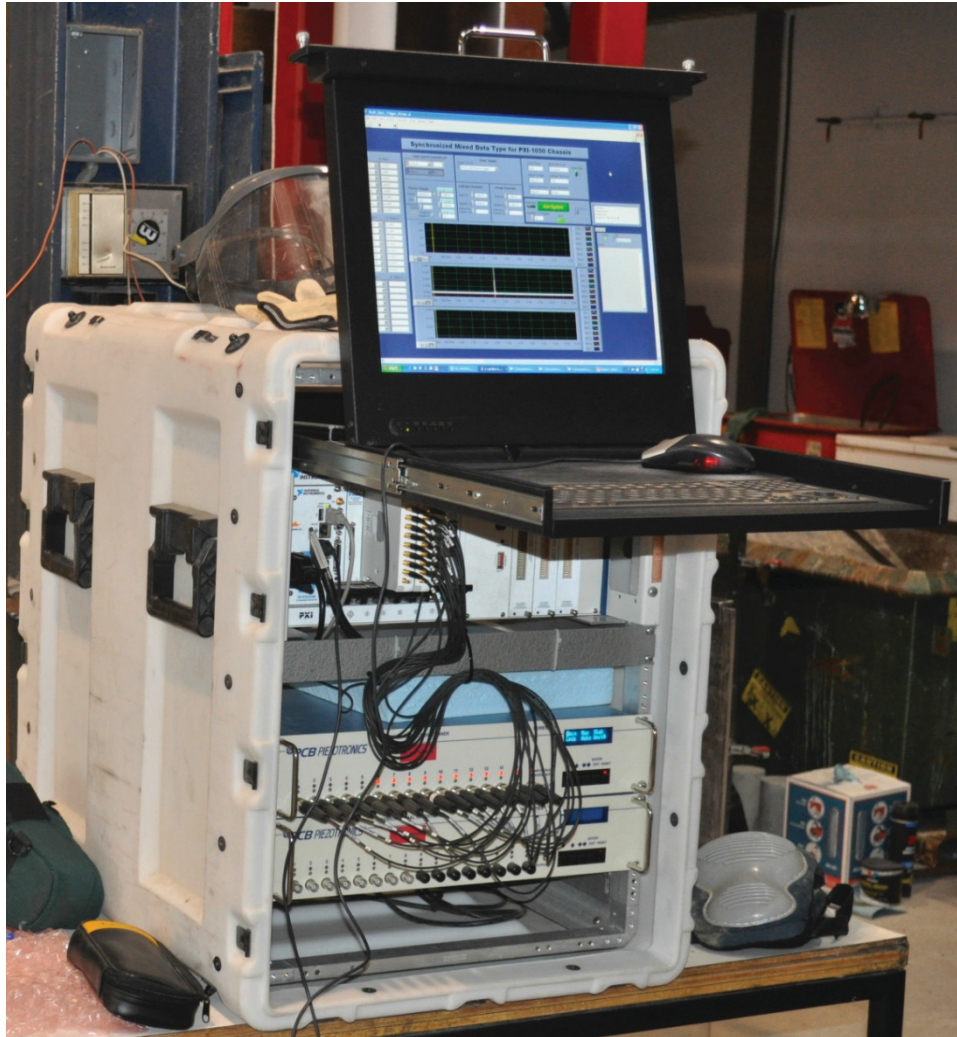


Figure 15 - Data Acquisition System

Table 1 - Data acquisition system details.

Description	Manufacturer	Model
Chassis	National Instruments	PXI-1050
Computer/Controller	National Instruments	PXI-8106
Digitizer	National Instruments	PXI-5105
Multifunction DAQ	National Instruments	PXI-6133
Strain Gauge-Module	National Instruments	SCXI-1520
Signal Conditioner	PCB	481A02
Dynamic Force Sensors	PCB	206C
Strain Gauges	Micro-Measurements	EA-06-10CBE-120 & EA-06-20CBW-120

Test Setup and Procedure

The test setup and procedure is described for the July 2011 and April 2012 dynamic tests. Details are also provided for the static tests that were performed in both July 2011 and April 2012.

July 2011 Dynamic Tests

In July 2011 dynamic tests were performed on concrete cylinders considering three parameters: test type, concrete composition and drop height. The test types included compression and tension, the composition was either normal weight concrete (NWC) or fiber reinforced concrete (FRC), and the drop weight was released from either 8 ft or 16 ft. All combinations of parameters were considered and tested as shown in Table 3.

Table 2 - Heating of Specimens

Specimen Type	Approximate Heating Time (hrs)	Specimen Type	Approximate Heating Time (hrs)	Specimen Type	Approximate Heating Time (hrs)
TF8-400	25.0	TF16-400	23.0	TF0-400	45.5
CF8-400	26.0	CF16-400	24.5	CF0-400	45.0
TN8-400	43.0	TN16-400**	44.0	TN0-400	45.0
CN8-400	53.0	CN16-400***	72.5	CN0-400	51.0
		CN16-cooled	49.0		

** TN16-400-4-1 was heated for 74 hours

*** CN16-400-4-1 was only heated for 54 hours

The cylinders were placed directly on top of the load cell system. For the tension test the cylinders were placed on their side directly in the middle of the five load cells as shown previously in Figure 7 and Figure 8. A wooden slat, similar to those used in static tests, was placed above and below the cylinders. Clay, or a small piece of aggregate, was used to stabilize the cylinders during tests and avoid rolling. For the compression tests the cylinders were placed in an upright position directly in the middle of three load cells to best distribute the load. The typical placement for compression tests was shown previously in Figure 9.

Prior to testing, trial tests were performed to determine what drop weight would be appropriate from a certain height. The drop weights listed in Table 3 were believed to achieve results that would best represent proper failure of the cylinders. At the time of testing, tension tests were of more interest than compression tests. For this reason, more tension tests were performed with this test type.

April 2012 Dynamic Tests

Additional tests at elevated temperatures, with parameters similar to those used in July 2011 tests, were performed in April 2012. The elevated temperature tests were not initially planned when the specimens were cast; therefore the quantity of fiber reinforced concrete cylinders was limited. Both normal weight and fiber reinforced concrete was tested at 400°F for each test type and drop height. The test matrix for the April 2012 dynamic tests is shown in Table 4. With the

use of the hemispherical plate for the April 2012 tests, the cylinders were simply placed centrally on top of the hemispherical plate as shown in Figure 16 and Figure 17.

Table 3 - July 2011 Dynamic Test Matrix

Specimen Notation	Number of Tests	Test Type	Composition	Drop Weight (lbf)	Drop Height (ft)
CN8	3	Compression	Normal Weight	92	8
CF8	3	Compression	Fiber Reinforced	158	8
CN16	3	Compression	Normal Weight	70.5	16
CF16	3	Compression	Normal Weight	92	16
TN8	8	Tension	Fiber Reinforced	70.5	8
TF8	9	Tension	Normal Weight	92	8
TN16	9	Tension	Normal Weight	49.5	16
TF16	7	Tension	Fiber Reinforced	49.5	16



Figure 16 – Specimen Placement for Dynamic Split Tension Tests



Figure 17 - Specimen Placement for Dynamic Compression Tests

Only NWC cylinders were tested for room temperature tests since FRC specimens were not available. Tests on the same specimen types were performed in July 2011; however, different drop weights were used. The drop weight was modified from the July 2011 test in an effort to be more representative of the static test procedure.

The change in drop weight was the reason for repeating the same room temperature tests in April 2012 that were performed in July 2011. Even though heated cylinders were not tested in July 2011 it was desirable to know what overall effects the change in drop weight would have on the results. Knowing the effects of the drop weight, it could be determined if it would be appropriate to make comparisons between the room temperature, FRC tests done in July 2011 with elevated temperature, and FRC tests done in April 2012 at different drop weights. An additional purpose for repeating tests at room temperature is the fact that concrete strength changes over time. For this reason room temperature static tests were also performed.

Table 4 - April 2012 Dynamic Test Matrix

Specimen Notation	Number of Tests	Test Type	Temperature	Composition	Drop Weight (lbf)	Drop Height (ft)
CN8-400	5	Compression	400°F	Normal Weight	223	8
CF8-400	3	Compression	400°F	Fiber Reinforced	223	8
CN8-R	3	Compression	Room	Normal Weight	223	8
CN16-400	5	Compression	400°F	Normal Weight	136	16
CF16-400	3	Compression	400°F	Fiber Reinforced	136	16
CN16-R	3	Compression	Room	Normal Weight	136	16
TN8-400	5	Tension	400°F	Normal Weight	92	8
TF8-400	3	Tension	400°F	Fiber Reinforced	92	8
TN8-R	3	Tension	Room	Normal Weight	92	8
TN16-400	5	Tension	400°F	Normal Weight	53.5	16
TF16-400	3	Tension	400°F	Fiber Reinforced	53.5	16
TN16-R	3	Tension	Room	Normal Weight	53.5	16

Table 5 - Change in Drop Weights

Specimen Type	Drop Weight (lbf)	
	July 2011	April 2012
CN8	92	223
CF8	158	
CN16	70.5	136
CF16	92	
TN8	70.5	92
TF8	92	

TN16	49.5	53.5
TF16	49.5	

The results from the July 2011 tests were such that the concrete did not break completely (see Appendix A for pictorial results). This was the case more so for the compression tests than for the tension tests. Therefore, the drop weights were increased significantly for the compression tests and slightly for the tensions tests. It was desirable for each specimen type, and for every height, to have the same drop weight for comparison purposes. For example, every compression test with a drop height of 8 ft had a drop weight of 223 pounds. Table 5 shows each test type and its corresponding drop weight for both July 2011 and April 2012 tests.

Static Testing

Static tests were performed to establish a basis for comparison with the dynamic drop hammer results. These tests were performed on the same day as the drop hammer tests to reduce variability in specimens. Static tests were performed for both compression and split tension on both normal weight and fiber reinforced concrete. Due to the limited number of FRC specimens available in April 2012, some static tests utilized 6 in. diameter by 12 in. high cylinders specimens so that all dynamic tests could be performed using 4 in. diameter by 8 in. high cylinders. The static test matrices are shown in Table 6 for the July 2011 and Table 7 for the April 2012 tests.

The configuration for the static compression test is shown in Figure 18. Two steel caps were placed on both ends of the cylinder to distribute the load evenly. The split tension tests were performed using a loading jig that held the cylinder on its side between two wood strips as shown in Figure 19. The loading jig held a steel rod directly over the center of the cylinder. A steel plate was then placed on top of the rod to distribute the load and achieve the desired split tension break.



Figure 18 - Static Compression Test



Figure 19 – Static Split Tension Test

Table 6 - July 2011 Static Test Matrix

Specimen Notation	Number of Tests	Test Type	Composition
CN	3	Compression	Normal Weight
CF	3	Compression	Fiber Reinforced
TN	3	Tension	Normal Weight
TF	3	Tension	Fiber Reinforced

Table 7 - April 2012 Static Test Matrix

Specimen Notation	Number of Tests	Test Type	Temperature	Composition
CN0-R	4	Compression	Room	Normal Weight
CF0-R*	3	Compression	Room	Fiber Reinforced
CN0-400	4	Compression	400°F	Normal Weight
CF0-400**	3	Compression	400°F	Fiber Reinforced
TN0-R	4	Tension	Room	Normal Weight
TF0-R*	3	Tension	Room	Fiber Reinforced
TN0-400	4	Tension	400°F	Normal Weight
TF0-400**	2	Tension	400°F	Fiber Reinforced

* All specimens were 6"x 12" Cylinder

** One of the specimens was a 6" x 12" Cylinder

July 2011 Dynamic Test Procedure

The procedure for the dynamic tests performed in July 2011 was as follows:

1. Test load cells and strain gauge connections periodically. Torque load cells or adjust strain gauge connections if necessary.
2. Prepare data acquisition and camera software.
3. Prepare drop hammer with appropriate weight and connect to electric cable hoist.
4. Connect strain gauges to the data acquisition system. Test wiring periodically with a volt meter to ensure correct readings are being recorded.
5. Raise the drop weight high enough to place the specimen centrally below the weight.
6. Place the cylinder with the correct orientation and in the correct location with respect to the load cell system.
7. Release the safety on the quick release hook and close the protective cage around the base of the drop hammer.
8. Raise drop weight to desired height.

9. Simultaneously begin data acquisition system, trigger camera and pull on quick release hook to drop weight.
10. Visually inspect and record break before removing specimen and debris.
11. Filter and save data collected from data acquisition system and high speed cameras.

April 2012 Dynamic Test Procedure

The procedure for the dynamic tests performed in April 2012 is listed below. Figure 20 through Figure 26 show visual implementation of the test procedure.

1. Test load cells and torque if necessary.
2. Prepare drop hammer with appropriate weight and connect to electric cable hoist.
3. Release the safety on the quick release hook and raise drop weight above safety bar location.
4. Insert safety bar into slotted pipe and raise weight to desired height.
5. Prepare data acquisition software.
6. Remove specimen from the oven and record temperature.
7. Place on cart and cover with Styrofoam box. Transport to drop hammer facility.
8. Place the cylinder in the correct orientation on the hemispherical plate and close the protective cage around the base of the drop hammer
9. Measure and record temperature.
10. Remove safety bar.
11. Simultaneously begin data acquisition system, trigger camera and pull on quick release hook to drop weight.
12. Visually inspect and record break before removing specimen and debris
13. Filter and save data collected from data acquisition system.

Static Test Procedure

The procedure for static tests performed in July 2011 and April 2012 is listed below. Handling of heated specimens for static tests followed the same procedure as outlined in the April 2012 dynamic test procedure.

1. Set the Satec™ series Instron® machine to the appropriate loading rate

2. Place cylinder on Instron platform.
 - a. For compression tests, place steel caps on the top and bottom of the cylinder.
 - b. For tension test, place the cylinder in the loading jig.
3. Close the protective cage.
4. Raise the Instron platform until a minimal load is applied.
5. Arm the Instron machine and begin test.
6. Visually inspect and record break before removing specimen and debris
7. Filter and save data collected from data acquisition system.

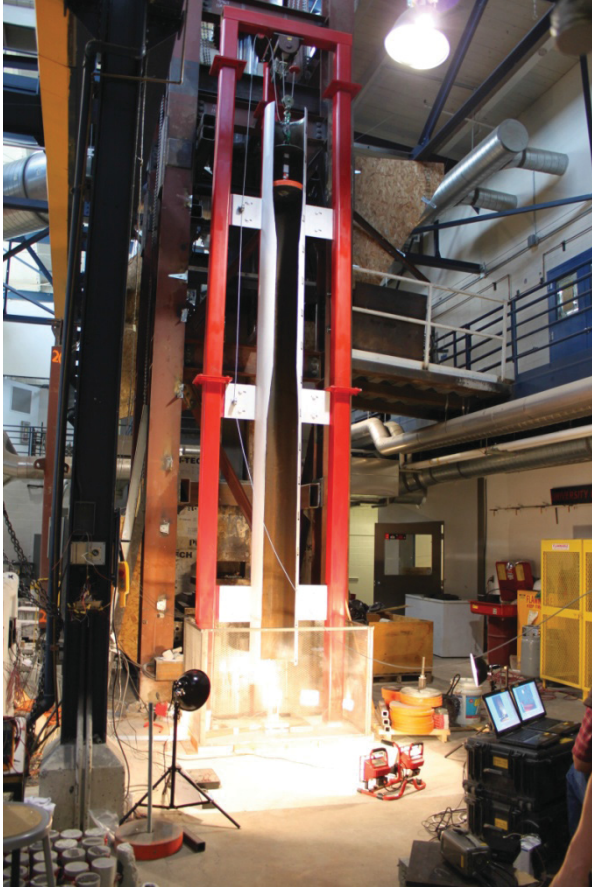


Figure 20 - Drop Hammer Facility Set Up



Figure 22 - Heated Cylinder



Figure 23 - Cylinder Transport



Figure 21 - Despatch Oven



Figure 24 - Cylinder Placement



Figure 25 - Temperature Reading

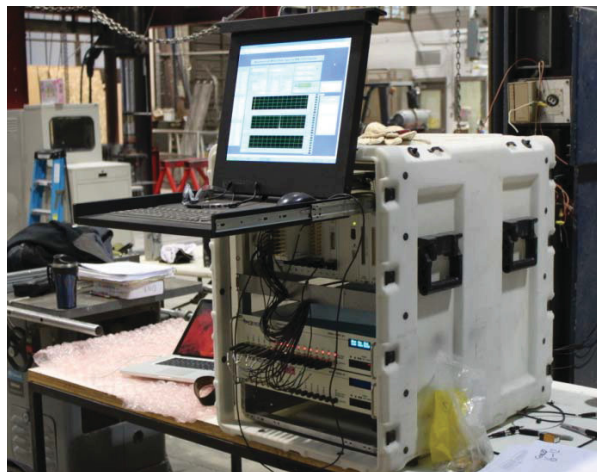


Figure 26 - Data Acquisition System

Data Reduction

Three software programs were used to reduce the information collected from the test equipment. Diadem, a National Instruments software, was used to reduce data collected from the data acquisition system, which recorded data from the load cells and strain gauges. A video review program was used to review high speed camera recordings and take measurements at given time increments. Partner Material Testing software was used to record data for the static tests performed on the Satec series Instron.

DIAdem

DIAdem version 11.1, a National Instruments software program⁵, was used to filter data collected from the data acquisition system. For each strain gauge, data was recorded for strain at a given point in time. For the load cells system, a load was recorded for each load sensor. A script was written in DIAdem that combined and filtered the five load sensors giving data for one load at a given point in time for each test.

Video Program

Phantom Cine Viewer v2.0 software⁶, which allows high speed videos to be played per frame, was used to measure how the cylinder dimensions changed over time. Frames could be viewed approximately every 10^{-4} seconds.

The Cine Viewer has tools that can be used to make measurements on a given frame. Initially, a calibration is made. For the tension test the diameter of the cylinder, and for the compression test the cylinder height were used to calibrate the measuring tool. The Cine Viewer also provides time information with accuracy of 10^{-6} second. Details about how the measurements tool and time were used to determine the strain rate in the Cine Viewer are discussed in the High Speed Camera Method section.

The measuring tool was also used to determine the velocity of the falling drop hammer. For the 8 ft drop hammer tests the average velocity was 21.2 ft/sec. For the 16 ft drop hammer tests the average velocity was 30.9 ft/sec.

Partner™ Material Testing

The program Partner™ Material Testing for Windows was used to operate and record data from the Satec™ Series Instron®. Partner records the load and corresponding time of the tests. By inputting the proper areas considering ASTM standard C496/C496M-04e1 for tension tests³ and C39/C39M -09a for compression tests⁴, the compressive strength and strain were calculated. The data recorded could be exported to an Excel file, which could be used for further analysis. This was done to determine the strain rates and to verify the compressive strength using the initial raw data of measured load and time.

Data Analysis

Three main methods of determining the strain rate were explored: the high speed camera method, the load cell method and the strain gauge method. Each method was reviewed to decide which method to consider.

High Speed Camera Method

During the July 2011 tests, high speed cameras were used to record the tests of each specimen. The high speed videos of the tests made it possible to visually see how the cylinder responded to dynamic loading. The breaking pattern for the different specimen types were better understood from the video recordings. The visual data collected provided information that was used in the high speed camera method of determining strain rates.

The strain rates were calculated by measuring the change in size of the specimen as it was tested. For the tension tests, measurements of the cylinder diameter were taken for each recorded frame, which occurred approximately every 10^{-4} seconds. The change in diameter as the cylinder broke apart was divided by the time in which the change occurred, giving the strain rate. For the compression tests, the same procedure was used by measuring the change in height of the cylinder as it decreased while being loaded dynamically.

The strain rates were computed until the specimen crushed to a point where the diameter or height could no longer be measured. On average, this lasted $1.5 * 10^{-3}$ seconds. Individual strain

rates were computed over this time range for each specimen. That is, a strain rate was computed every 10^{-4} seconds for $1.5 * 10^{-3}$ seconds. The maximum strain rate, which was considered to be the strain rate of the concrete specimen, generally occurred within $0.75 * 10^{-3}$ seconds.

The high speed camera method introduces some error when measuring the width or height of the specimen. This was especially true for the compression tests which were difficult to measure because the drop weight obstructed the image of the cylinder. Also, the strain rate will be different depending on which location on the cylinder the measurement is made. Generally, the center of the specimen was found to better represent the specimen; however, it is difficult to insure that all measurements use the same portion of the cylinder as it breaks. Measuring the change in length on the end (considered for tension tests) or side (considered for compression tests) of the specimen corresponds to a local strain rate. Therefore, the high speed camera method does not represent the overall strain rate of the specimen.

Load Cell Method

The load cell method considers the data collected from the load cells and then applies elastic theory to determine the strain rate for each specimen. The first step in this method is to determine the loading rate. This was done by plotting the filtered load data. For example, Figure 27 shows the filtered load versus time data for a fiber reinforced specimen tested in tension at a drop height of 16 ft (TF16). The load versus time data for the July 2011 tests are given in Appendix B, and for the April 2012 tests in Appendix E. These figures show the individual loads for each load sensor, the total load for all load sensors and the filtered load, which was considered during analysis. The only portion of the graph considered was from initial loading to peak load. The point of initial loading was not always definitive and required some judgment as to where it should begin.

To determine the loading rate, various methods were explored. First, the loading rate in-between each data point was determined. For this approach, the loading rate was considered to be the average of the individual loading rates. Second, a linear regression line was computed, in which the loading rate was taken as the slope of the regression line. Lastly, only the maximum value of the individual loading rates in-between each data point was determined. The first two methods depend on the point of initial loading; the last method does not, making it a more standardized approach. Using the maximum value also proved to be the most consistent among the various tests, therefore, this was the approach used to determine the loading rate for all specimens.

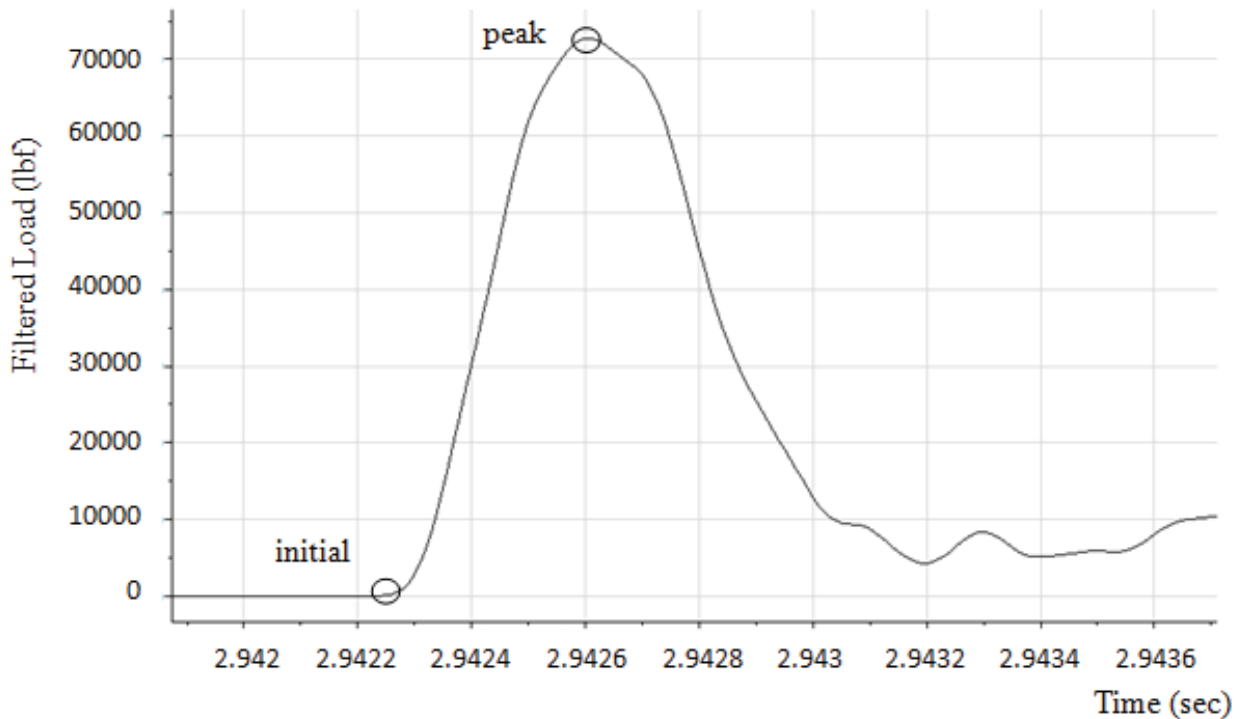


Figure 27 - TF16 Load Data

Once the loading rate (P_R) was determined, elasticity theory was applied. This method assumes that the relationship between stress and strain is linear. To compute the strain rate the compressive strength (f_c') was determined for NWC and FRC specimens. For the July 2011 tests the average compressive strength for CN and CF static tests were computed. For the April 2012, the average compressive strength for CF0-R and CN0-R were computed. These compressive strengths are from the room temperature, compressive static tests, which are most representative of the concrete material and can be used to determine the modulus of elasticity. Assuming the weight of concrete to be normal weight (145 pcf), and f_c' is given in ksi units, Equation (3) was used to determine the modulus of elasticity for NWC and FRC for both July 2011 and April 2012 tests.

$$E_c = 1746 \sqrt{f_c'} \quad (3)$$

The stress rate was then determined using the measured loading rate and the appropriate area according to ASTM standard C496/C496M-04e1 Standard Test Method for Splitting Strength of Cylindrical Concrete Specimens³ and C39/C39M -09a Standard Test Method for Compressive Strength of Cylindrical Concrete⁴. The area used for tension is half of the side surface area as shown in Figure 28 (a). The area used for compression is the cross sectional area of the cylinder as shown in Figure 28 (b). The stress rate was then determined using the calculated modulus of elasticity and appropriate area. Equation (4) was used for the tension tests and Equation (5) was used for the compression tests. For both equations, D is the cylinder diameter and L is the cylinder height; these equations give the stress rate in (ksi/in.). Finally, stress-strain properties were used to determine the strain rate in (in./in./sec) using Equation (6).

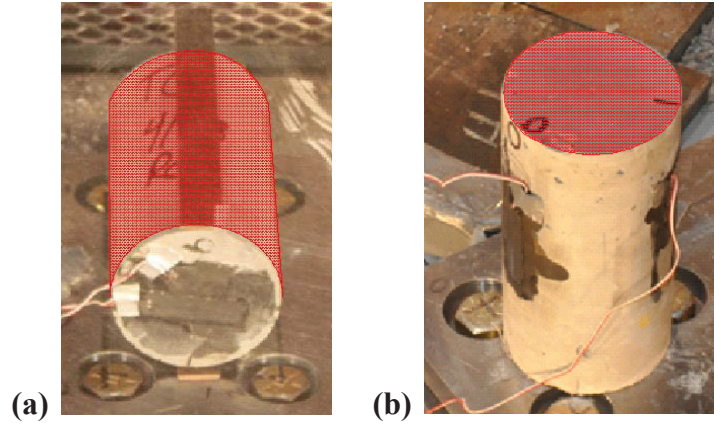


Figure 28 - Area Considered for (a) Tension and (b) Compression

$$\sigma_{R,Tension} = \frac{P_R}{A_{Tension}} = \frac{P_R}{(\pi * D * L)/2} \quad (4)$$

$$\sigma_{R,Compression} = \frac{P_R}{A_{Compression}} = \frac{P_R}{(\pi * D^2)/4} \quad (5)$$

$$\varepsilon_R = \frac{\sigma_R}{E_c} \quad (6)$$

Strain Gauge Method

Depending on the specimen type, compression versus tension test and 16 ft versus 8 ft drop, the strain gauge data varied greatly. Examples of different plots of strain versus time are shown in Figure 29 through Figure 33. Appendix C shows strain graphs for each specimen type.

Some approaches initially taken included: using a moving average from the initial strain to the peak, using an average of the moving average of the first and second portions (shown in Figure 29), using an overall average from initial to peak strain, and using the average of the two slopes where the plot changes from the first to the second portion. In some tests, different approaches were taken depending on the type of data available. The various methods used produced drastically different results within a single specimen and were not repeatable for any given specimen type.

After considering the load cell and high speed camera methods, it was observed that the peak plateau seen in a majority of the strain data was a result of the strain gauge reaching capacity. It was also determined that the data collected, after the strain began to decrease, was representative of the strain rate. For this reason, two new methods for determining the strain rate were considered. First, the strain rate was taken from the point in time when the strain began increasing significantly, all the way to the peak strain. Similarly, the strain rate was determined using the strain rate of the decreasing strain after the plateau was reached. The average of the absolute value of the two strain rates before and after the plateau was then considered to be the true strain rate.

The second method also considered the strain rates before and after the plateau. However, it considered the absolute average of single strain rates one data point prior to and after the plateau. That is, it only considered the second portion of the data. Both of these methods required judgment to determine which time values should be considered and which peak values were most appropriate in cases where the strain gauge did not reach capacity (when there was no plateau). There were also graphs that varied greatly as was shown in Figure 29 through Figure 33. This made it difficult to take a singular and consistent approach in the analysis of the data. However, the first approach had the most consistent results and was determined to be the best method; it was used to determine the strain rate.

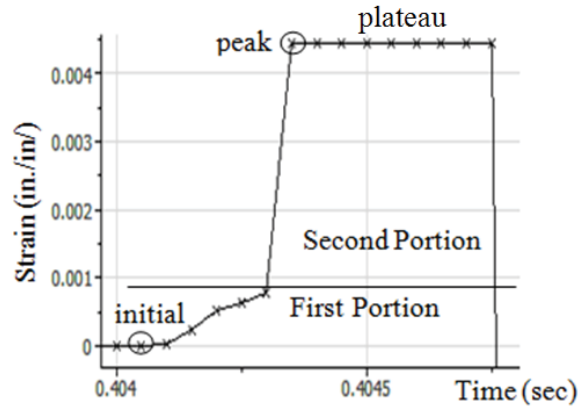


Figure 29 – TF16 Strain Data

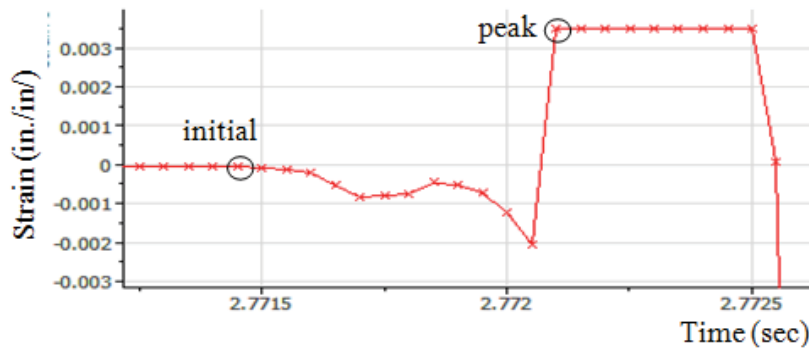


Figure 30 - CF16 Strain Data

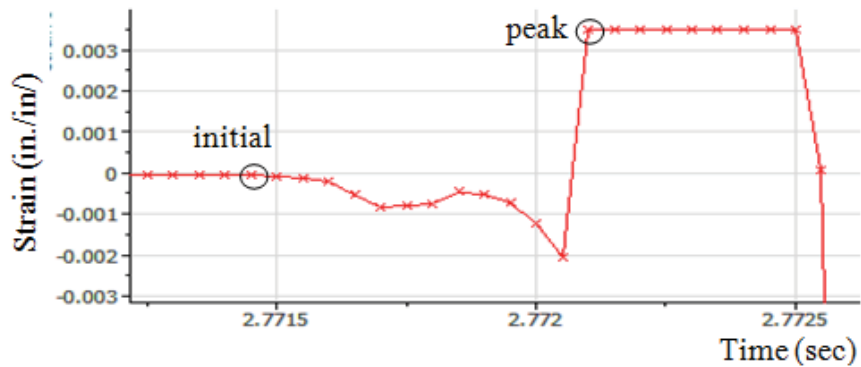


Figure 31 - CF16 Strain Data

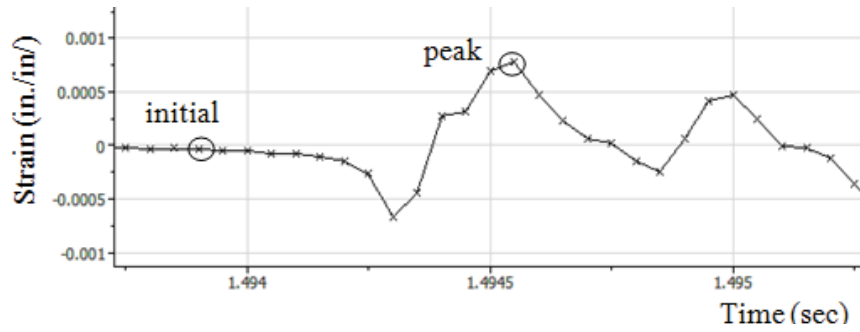


Figure 32 - CN16 Strain Data

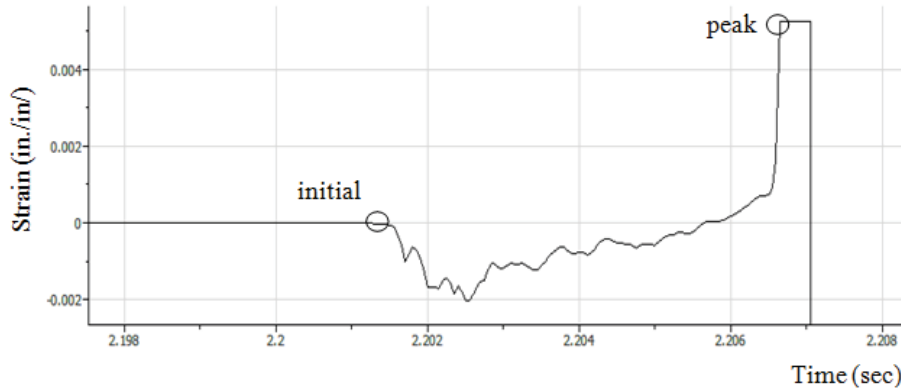


Figure 33 - CF8 Strain Data

Once refined, comparisons between the three methods of determining strain rates were made. Values determined for each method are shown in Table 8 for tests with an 8 ft test height. Tests done with a 16 ft test height are shown in Table 8. These results are also shown graphically in Figure 34, which is a plot of strain rates versus the ratio of dynamic to static load.

From Figure 34 it can be seen that the strain gauge and high speed camera methods for determining the strain rate produced very similar results. This is expected, since both methods represent a local strain rate measured at a similar location on the cylinder. The load cell method had strain rates that were significantly lower than the other two methods. It was also the method that best represented the cylinder as a whole. As a whole, the cylinder would be able to better resist the dynamic impact, thus having a lower strain rate.

For the purpose of these tests, a global representation of the dynamic impact effect is desired. Therefore, the load cell method was used to further analyze the effects of reinforcement and temperature under dynamic loading.

Table 8 – Comparison of Strain Rate Methods for 8 ft Drop Height

Specimen	Strain Rates (1/sec)				Maximum Filtered Load vs. Average Static Load
	Camera	Strain Gauge 0	Strain Gauge 1	Load Cells	
TF8-1	94	N.A.	N.A.	N.A.	N.A.
TF8-2	95	385	201	1.411	2.432
TF8-3	65	199	199	1.165	2.305
TF8-4	63	386	318	1.115	2.303
TF8-5	95	390	751	1.159	2.348
TF8-6	62	197	N.A.	0.868	1.922
TF8-7	95	N.A.	206	1.105	1.932
TF8-8	63	64	388	1.103	1.812
TF8-9	95	387	N.A.	1.223	1.852
CF8-1	51	308	N.A.	2.206	0.646
CF8-2	25	378	N.A.	4.152	0.568
CF8-3	47	N.A.	202	4.961	0.647
TN8-1	94	208	208	0.512	1.500
TN8-2	126	193	193	0.548	1.987
TN8-3	119	192	192	1.111	2.670
TN8-4	94	200	200	0.872	2.563
TN8-5	95	386	385	0.610	2.768
TN8-6	158	202	202	0.697	2.211
TN8-7	95	198	198	0.883	2.553
TN8-8	94	389	387	0.941	2.546
CN8-1	N.A.	216	N.A.	0.886	0.322
CN8-2	47	392	N.A.	3.152	0.412
CN8-3	31	235	235	1.881	0.416

Table 9 – Comparison of Strain Rate Methods for 16 ft Drop Height

Specimen	Strain Rates (1/sec)				Maximum Filtered Load vs. Average Static Load
	Camera	Strain Gauge 0	Strain Gauge 1	Load Cells	
TF16-1	95	201	204	0.619	1.621
TF16-2	95	196	N.A.	1.274	2.384
TF16-3	127	386	N.A.	1.225	2.243
TF16-4	96	386	200	1.541	2.694
TF16-5	95	383	198	1.096	2.307
TF16-6	94	202	368	1.237	2.109
TF16-7	95	389	391	0.755	1.766
CF16-1	47	191	191	5.293	0.749
CF16-2	19	252	N.A.	9.429	0.866
CF16-3	48	209	243	5.551	0.704
TN16-1	157	388	N.A.	0.845	2.310
TN16-2	126	202	235	1.780	4.031
TN16-3	95	202	392	1.231	4.124
TN16-4	94	379	193	1.599	3.757
TN16-6	157	N.A.	N.A.	N.A.	N.A.
TN16-7	119	214	209	N.A.	N.A.
TN16-8	95	217	204	1.339	2.970
TN16-9	125	199	200	1.112	3.262
CN16-1	46	209	N.A.	3.761	0.530
CN16-2	24	543	203	4.945	0.683
CN16-3	47	342	363	5.259	0.682

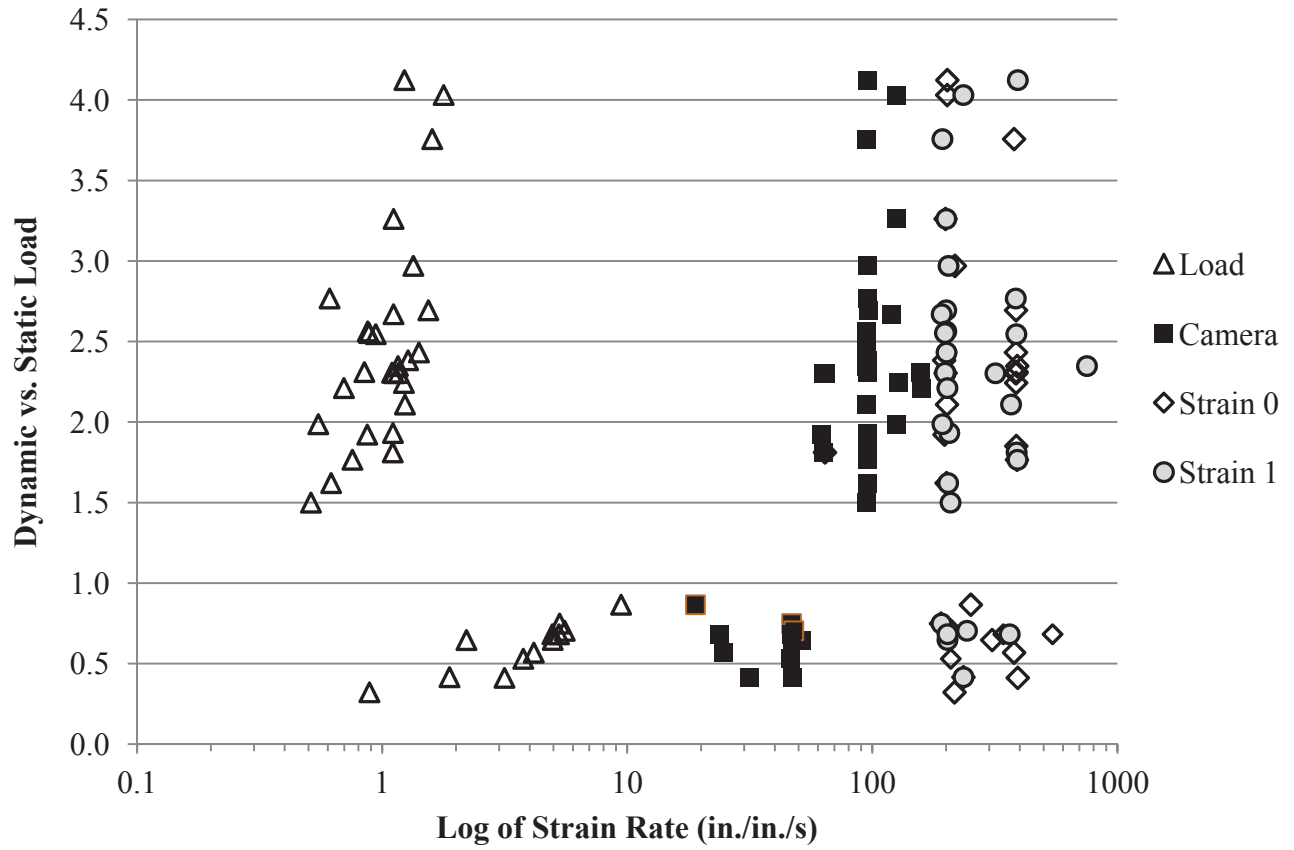


Figure 34 – Comparison of Strain Rate Methods

Results

For several of the tests, comparisons were made when different drop weights were used. To evaluate the effect of the drop weight, the NWC room temperature tests from July 2011 were compared to the same tests performed in April 2012. For all tests the drop weights were increased from July 2011 to April 2012. The compression tests in July 2011 had a compressive strength of 10,900 psi, whereas the April 2012 tests had a compressive strength of 11,000 psi. Similarly, the tension test strengths were 520 psi in July 2011 and 470 psi in April 2012. The strength of the concrete did not change significantly between the two test dates and is therefore not considered to be a variable. Similar results were also found for the FRC specimens.

The CN8 test drop weights increased from 92 to 223 lbf. The average DIF increased from 0.4 during July 2011 to 0.5 during April 2012. The average strain rate also increased from 2.0 to 3.1 in./in./sec. For the CN16 specimens the drop weight increased from 70.5 to 136 lbf in April 2012. The average DIF increased from 0.6 to 1.0 and the average strain rate increased from 4.7 to 9.0 in./in./sec.

The changes in drop weight for the tension tests were less extensive than the compression tests. For TN8 tests the drop weight increased from 70.5 to 92 lbf. This decreased the average DIF from 2.4 to 1.4 and the average strain rate from 0.8 to 0.6 in./in./sec. For the TN8 tests the drop

weight increased from 49.5 to 53.5 lbf. This decreased the DIF from 3.4 to 2.2 and the average strain rate from 1.3 to 0.9 in./in./sec.

The result of increasing the drop weight by 142% for the CN8 tests had a similar effect as increasing the drop weight by 8% for the TN16 tests. Since a direct correlation between drop weights and resulting DIF and strain rates were not observed between the July 2011 and April 2012, test types with different drop weight are believed to be comparable. However, the drop weights are noted when comparing test results to demonstrate the different testing conditions. It is also noted that the change in drop weight had a larger effect on the strain rate than on the DIF.

To summarize the dynamic test results, the DIFs are compared visually with the strain rates in Figure 35 for the July 2011 tests and in Figure 36 for the April 2012 tests. Similar drop hammer research has been conducted to determine the relationship between strain rate and DIF, a summary of which is shown in Figure 37. Malvar and Ross⁷ compare the results from several dynamic impact tension tests using different loading procedures on various specimen sizes. Mellinger and Birkimer tested 10.25 in. long by 2 in. diameter specimens, Birkimer tested 35 in. long by 2 in. diameter specimens, and Ross tested specimens with diameters ranging from 0.75 to 2 in. and length ranging from 2 to 3 in.

In addition, Millar, Molyneaux and Barnett⁸ performed dynamic flexural and shear tests on 11.0 by 2.8 by 2.8 in. beams and 13.8 by 3.9 by 2.0 in. beams. A summary of their results is shown in Figure 38. All previous research found regarding dynamic impact factors on concrete used various specimen sizes. No other drop hammer tests used 4 in. diameter by 8 in. long cylinders.

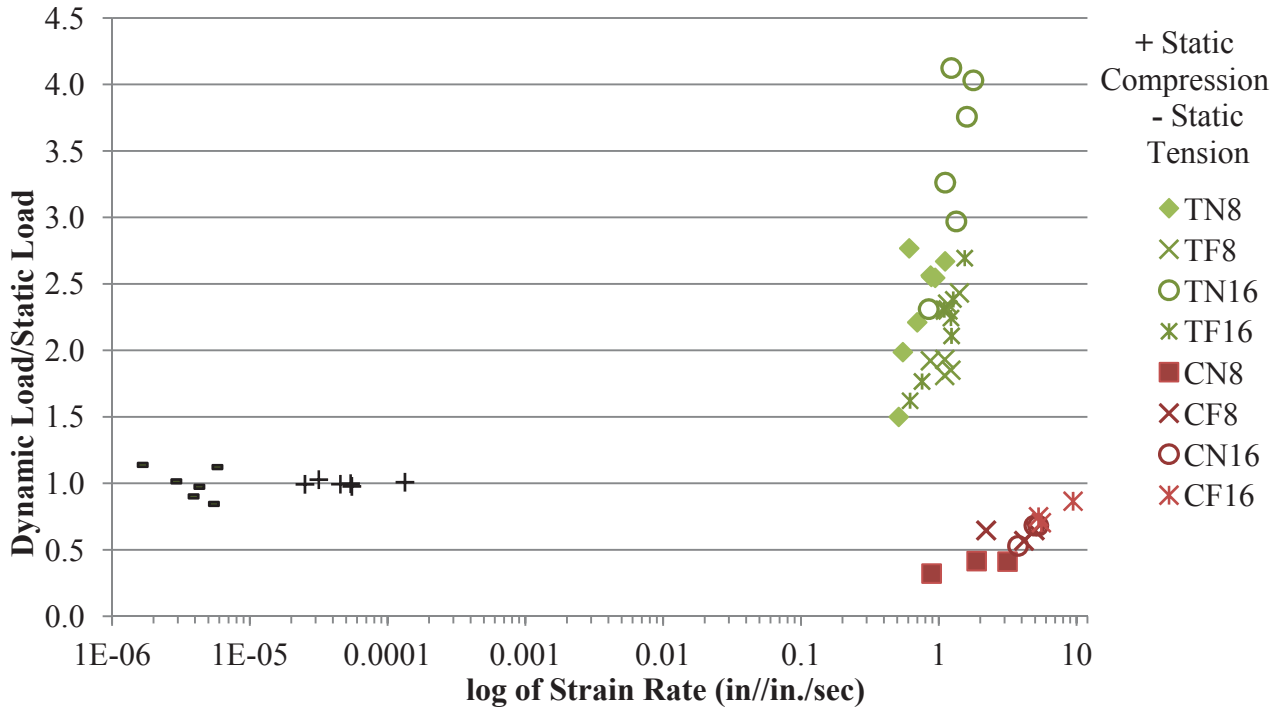


Figure 35 - Dynamic Increase Factor vs. Strain Rate for July 2011

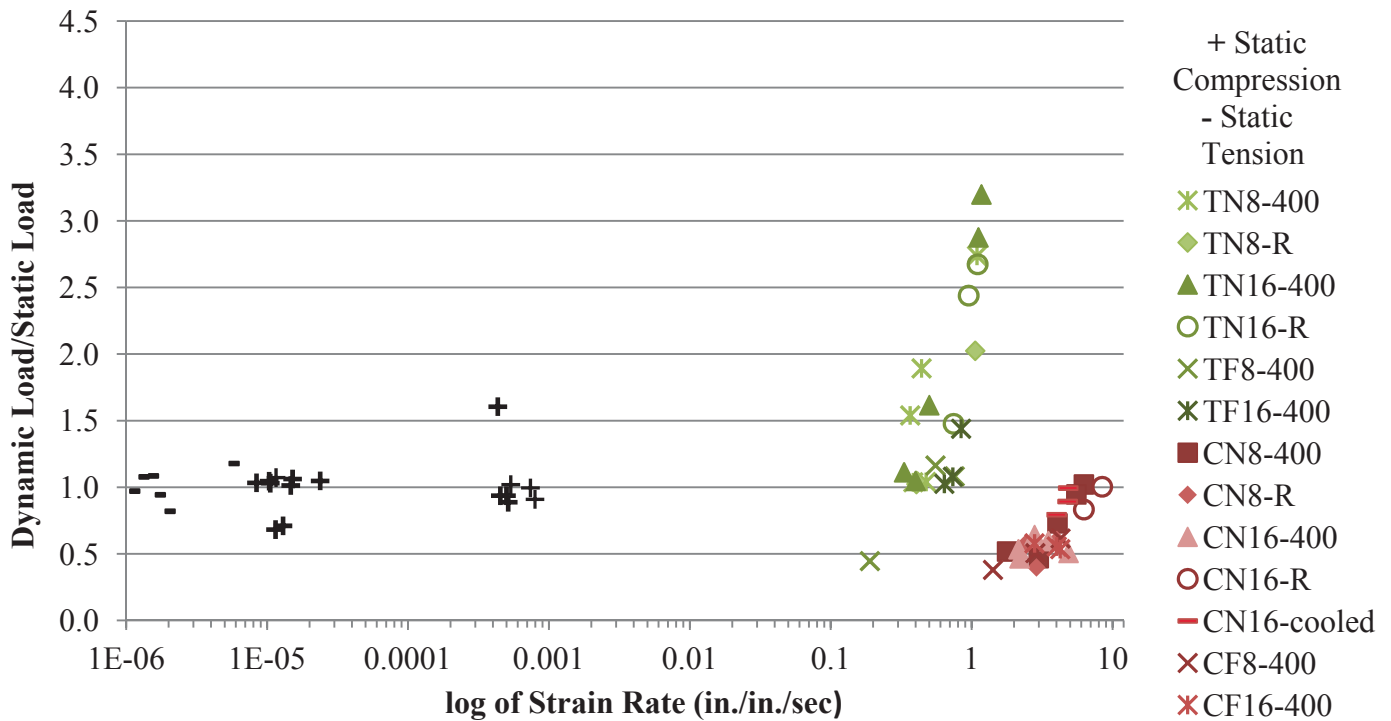


Figure 36 - Dynamic Increase Factor vs. Strain Rate for April 2012

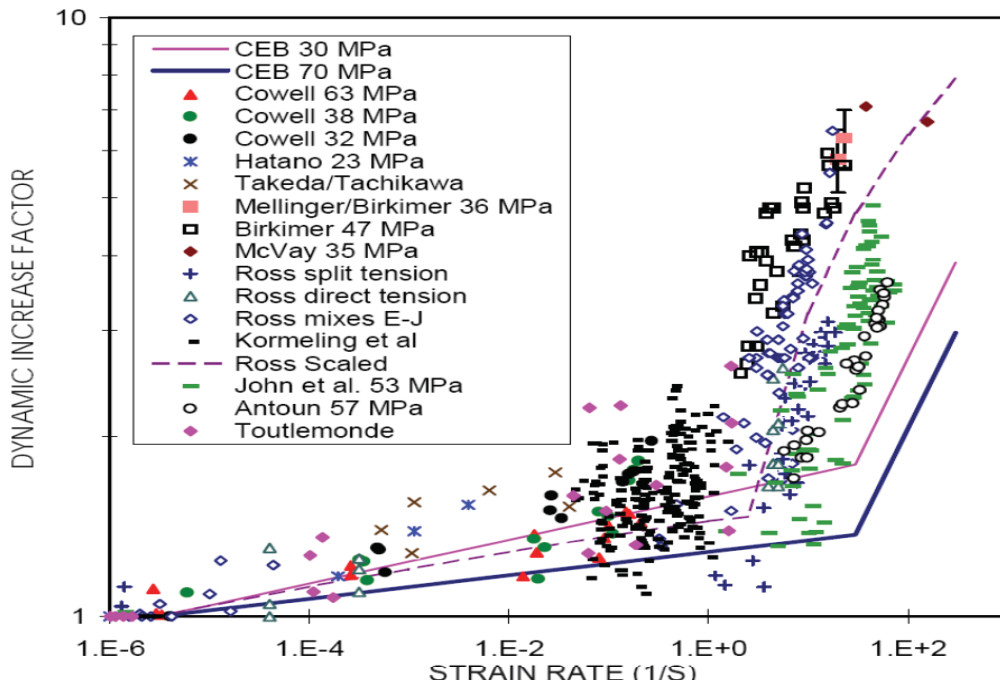


Figure 37 – Malvar and Ross’s Comparison of Strain Rate Effects for Concrete in Tension⁷

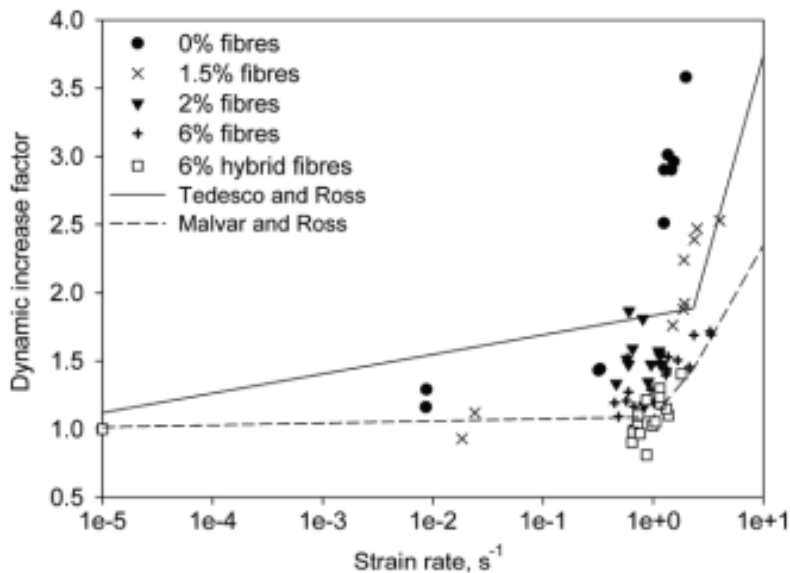


Figure 38 – Millard, Molyneaux and Barnett’s Dynamic Increase Factor of Maximum Load with Strain⁸

To review the results of the drop hammer tests more extensively, comparisons were made between drop heights of 8 ft and 16 ft for NWC and FRC at room temperature and between drop height of 8 ft and 16 ft for NWC and FRC at elevated temperatures. Comparisons were also made between NWC and FRC at room temperature and between NWC and FRC at elevated temperatures. Finally, comparisons were made between room and elevated temperatures for both NWC and FRC. For each dynamic tests specimen type, load versus time data is shown in Appendix B for July 2011 and in Appendix E for April 2012 tests. Appendix A and D also provide visual results for July 2011 and April 2012 static and dynamic tests.

Drop Height at Room Temperature

Results for the July 2011 tests are shown in Table 10 for static tests, and Table 11 for dynamic tests with an 8 ft drop height and Table 12 for dynamic tests with a 16 ft drop height. To determine the effect of the drop height at room temperature, NWC concrete specimens are compared. The TN8 specimens, with a 70.5 lbf drop weight, had an average strain rate of 0.8 in./in./sec (range of 0.5 to 1.1 in./in./sec). For the TN16 specimens (49.5 lbf drop weight) the average strain rate increased to 1.3 in./in./sec (range of 0.8 to 1.8 in./in./sec). The TN8 tests had an average DIF of 2.4 (range of 1.5 to 2.8), which also increased to 3.4 (ranging from 2.3 to 4.1) for the TN16 specimens.

The CN8 specimens, with a 92 lbf drop weight, had an average strain rate of 2.0 in./in./sec (range of 0.9 to 3.2 in./in./sec). For the CN16 specimens (70.5 lbf drop weight) the average strain rate increased to 4.7 in./in./sec (ranging from 3.8 to 5.3). The CN8 specimens had an average DIF of 0.4 (ranging from 0.3 to 0.4) which increased to 0.6 (ranging from 0.5 to 0.7) for the CN16 specimens.

Increasing the drop height from 8 ft to 16 ft resulted in a higher average strain rate for NWC tests. Increasing the drop height had a greater effect on the strain rates of the compression tests which increased by 135%, than the tension tests which increased by 63%. The DIF for both tension and compression tests increased by approximately 50% when the drop height was doubled.

The change in drop height is also compared for FRC specimens. The TF8 specimens, with a 70.5 lbf drop weight, had an average strain rate of 1.1 in./in./sec (range of 0.9 to 1.4 in./in./sec). The TF16 specimens (49.5 lbf drop weight) had the same average strain rate of 1.1 in./in./sec (range of 0.6 to 1.5 in./in./sec). The DIFs were also very similar: the average DIF for the TF8 specimen was 2.1 (range of 1.8 to 2.4) and for the TF16 specimen it was 2.2 (range of 1.6 to 2.7).

The CF8 specimens, with a 158 lbf drop weight, had an average strain rate of 3.8 in./in./sec (range of 2.2 to 5.0 in./in./sec). For the CN16 specimens (70.5 lbf drop weight) the average strain rate increased to 6.8 in./in./sec (ranging from 5.3 to 9.4). The CF8 specimens had an average DIF of 0.6 (ranging from 0.6 to 0.6). The CF16 specimens had an average DIF of 0.8 (ranging from 0.7 to 0.9).

For the FRC tension specimen, increasing the drop height from 8 ft to 16 ft had little effect on the average strain rate and DIF. However, the FRC compression tests were affected by the change in drop height. The average strain rate increased by approximately 80% and the DIF increased by approximately 30% with an increase in drop height from 8 ft to 16 ft.

Table 10 - July 2011, Static Test Results

Specimen ID	Strain Rates (in/in/sec)	Compressive Strength (psi)	Maximum Load (lbf)	Maximum Load/Maximum Average Load
TF-1	3.97E-06	592	29737	0.975
TF-2	5.37E-06	682	34260	1.123
TF-3	3.61E-06	548	27531	0.902
Average		607	30509	
CF-1	5.49E-05	9706	121971	0.978
CF-2	4.53E-05	9863	123948	0.994
CF-3	3.16E-05	10207	128268	1.028
Average		9926	124729	
TN-1	5.07E-06	399	20071	0.846
TN-2	2.70E-06	479	24093	1.015
TN-3	1.54E-06	538	27024	1.139
Average		472	23729	
CN-1	1.34E-04	11130	139859	1.009
CN-2	2.51E-05	10951	137620	0.993
CN-3	5.38E-05	11008	138336	0.998
Average		11030	138605	

Table 11 - July 2011, 8 ft Test Results

Specimen ID	Strain Rate (in./in./sec)	Maximum Dynamic Load (lbf)	Average Maximum Static Load (lbf)	Dynamic/Static Load
TF8-1	N.A.	N.A.	30509.3	N.A.
TF8-2	1.411	74207		2.432
TF8-3	1.165	70312		2.305
TF8-4	1.115	70267		2.303
TF8-5	1.159	71637		2.348
TF8-6	0.868	58642		1.922
TF8-7	1.105	58950		1.932
TF8-8	1.103	55272		1.812
TF8-9	1.223	56488		1.852
CF8-1	2.206	80629	124728.7	0.646
CF8-2	4.152	70883		0.568
CF8-3	4.961	80755		0.647
TN8-1	0.512	35595	23729.3	1.500
TN8-2	0.548	47150		1.987
TN8-3	1.111	63353		2.670
TN8-4	0.872	60822		2.563
TN8-5	0.610	65674		2.768
TN8-6	0.697	52474		2.211
TN8-7	0.883	60578		2.553
TN8-8	0.941	60412		2.546
CN8-1	0.886	44634	138604.7	0.322
CN8-2	3.152	57063		0.412
CN8-3	1.881	57661		0.416

Table 12 - July 2011, 16 ft Test Results

Specimen ID	Strain Rate (in./in./sec)	Maximum Dynamic Load (lbf)	Average Maximum Static Load (lbf)	Dynamic/Static Load
TF16-1	0.619	49465	30509	1.621
TF16-2	1.274	72727		2.384
TF16-3	1.225	68444		2.243
TF16-4	1.541	82205		2.694
TF16-5	1.096	70384		2.307
TF16-6	1.237	64349		2.109
TF16-7	0.755	53882		1.766
CF16-1	5.293	93409	124729	0.749
CF16-2	9.429	108006		0.866
CF16-3	5.551	87833		0.704
TN16-1	0.845	54825	23729	2.310
TN16-2	1.780	95652		4.031
TN16-3	1.231	97850		4.124
TN16-4	1.599	89158		3.757
TN16-6	N.A.	N.A.		N.A.
TN16-7	N.A.	N.A.		N.A.
TN16-8	1.339	70477		2.970
TN16-9	1.112	77400		3.262
CN16-1	3.761	73496		138605
CN16-2	4.945	94661	0.683	
CN16-3	5.259	94585	0.682	

Drop Height at Elevated Temperature

Results for the April 2012 tests are shown in Table 13 for static tests, and Table 14 for dynamic tests with an 8 ft drop height and Table 15 for dynamic tests with a 16 ft drop height. To determine the effects of the drop height at elevated temperature, NWC concrete specimens are compared. The TN8-400 specimens, with a 92 lbf drop weight, had an average strain rate of 0.5 in./in./sec (range of 0.4 to 1.1 in./in./sec). For the TN16-400 specimens (53.5 lbf drop weight) the average strain rate increased to 0.7 in./in./sec (range of 0.3 to 1.2 in./in./sec). The TN8-400 tests had an average DIF of 1.7 (range of 1.0 to 2.7), which increased to 2.0 (ranging from 1.0 to 3.2) for the TN16 specimens.

The CN8-400 specimens, with a 223 lbf drop weight, had an average strain rate of 4.1 in./in./sec (range of 1.8 to 6.3 in./in./sec). For the CN16-400 specimens (136 lbf drop weight) the average strain rate decreased to 3.1 in./in./sec (ranging from 2.1 to 4.9). The CN8-400 tests had an average DIF of 0.7 (ranging from 0.5 to 1.0) which decreased to 0.6 (ranging from 0.5 to 0.6) for the CN16-400 specimens.

Increasing the drop height from 8 ft to 16 ft resulted in higher average strain rates for elevated temperature, NWC tension specimens, which increased by 40%. However, the average strain rates for the elevated temperature, NWC compression tests decreased by 25% when the drop height was increased. The change in drop height did not have as large of an effect on the elevated temperature DIFs, which increased 18% for NWC tension tests and decreased by 14% for NWC compression tests.

The change in drop height is also compared for elevated temperature FRC specimens. The TF8-400 specimens, with a 92 lbf drop weight, had an average strain rate of 0.5 in./in./sec (range of 0.2 to 0.8 in./in./sec). For the TF16-400 specimens (53.5 lbf drop weight) the average strain rate increased to 0.7 in./in./sec (range of 0.6 to 0.8 in./in./sec). The DIFs also increased from 0.9 (range of 0.5 to 1.1) for the TF8-400 specimens to 1.2 (range of 1.1 to 1.4) for the TF16-400 specimens.

The CF8-400 specimens, with a 223 lbf drop weight, had an average strain rate of 2.8 in./in./sec (range of 1.4 to 4.3 in./in./sec). For the CN16-400 specimens (136 lbf drop weight) the average strain rate increased to 3.7 in./in./sec (ranging from 2.8 to 4.3). The DIF also increased from 0.5 (ranging from 0.4 to 0.6) for the CF8-400 specimens to 0.6 (ranging from 0.5 to 0.6) for the CF16-400 specimens.

For the elevated FRC specimens, both the tension and compression tests had similar results when the drop height was increased. The compression tests were slightly less affected by the increased drop height with an increase in average strain rate of 32% and average DIF of 20%. The tension tests had a larger increase in average strain rate of 40% and average DIF of 33%.

Table 13 - April 2012, Static Test Results

Specimen ID	Strain Rates (in/in/sec)	Compressive Strength (psi)	Maximum Load (lbf)	Maximum Load/Maximum Average Load
TF0-400-4-1	1.90E-06	541	27173	0.821
TF0-400-6-1	5.40E-06	345	39028	1.179
Average		443	33101	
TF0-R-6-1	1.06E-06	588	66462	0.972
TF0-R-6-2	6.62E-07	574	64951	0.949
TF0-R-6-3	6.32E-07	653	73822	1.079
Average		605	68412	
CF0-400-4-1	1.15E-05	5107	64182	0.683
CF0-400-4-2	1.29E-05	5316	66806	0.711
CF0-400-6-1	4.33E-04	5336	150882	1.606
Average		5253	93957	
CF0-R-6-1	1.47E-05	9468	267711	1.014
CF0-R-6-2	2.37E-05	9791	276834	1.048
CF0-R-6-3	4.99E-04	8756	247565	0.938
Average		9338	264037	
TN0-400-4-1	1.45E-06	430	21637	1.086
TN0-400-4-2	1.62E-06	374	18811	0.944
TN0-400-4-3	1.24E-06	428	21505	1.079
TN0-400-4-4	8.60E-07	353	17764	0.891
Average		396	19929	
TN0-R-4-1	1.07E-06	525	26375	1.008
TN0-R-4-2	1.41E-06	548	27554	1.053
TN0-R-4-3	1.69E-06	513	25786	0.985
TN0-R-4-4	1.28E-06	496	24956	0.954
Average		521	26168	
CN0-400-4-1	1.03E-05	8270	103929	1.046
CN0-400-4-2	1.05E-05	8154	102467	1.032
CN0-400-4-3	5.13E-04	7021	88232	0.888
CN0-400-4-4	8.40E-06	8174	102723	1.034
Average		7905	99338	
CN0-R-4-1	7.95E-04	9939	124897	0.910
CN0-R-4-2	7.39E-04	10872	136628	0.996
CN0-R-4-3	5.36E-04	11145	140057	1.021
CN0-R-4-4	1.16E-05	11718	147248	1.073
Average		10919	137207	
CN0-cooled-4-1	4.51E-04	8194	102975	0.937
CN0-cooled-4-2	1.51E-05	9294	116796	1.063
Average		8744	109885	

Table 14 - April 2012, 8 ft Test Results

Specimen ID	Strain Rate (in./in./sec)	Maximum Dynamic Load (lbf)	Average Maximum Static Load (lbf)	Dynamic/Static Load
TF8-400-4-1	0.757	35821	33101	1.082
TF8-400-4-2	0.189	14770		0.446
TF8-400-4-3	0.553	38541		1.164
CF8-400-4-1	2.829	47549	93957	0.506
CF8-400-4-2	1.415	35723		0.380
CF8-400-4-3	4.271	57847		0.616
TN8-400-4-1	0.366	30687	19929	1.540
TN8-400-4-2	0.385	20689		1.038
TN8-400-4-3	0.441	37728		1.893
TN8-400-4-4	0.475	20738		1.041
TN8-400-4-5	1.090	54574		2.738
TN8-0-4-1	0.405	26799	26168	1.024
TN8-0-4-2	1.059	52990		2.025
TN8-0-4-3	0.406	27420		1.048
CN8-400-4-1	6.251	101491	99338	1.022
CN8-400-4-2	1.781	51476		0.518
CN8-400-4-3	5.530	94046		0.947
CN8-400-4-4	4.060	72496		0.730
CN8-400-4-5	2.987	46496		0.468
CN8-0-4-1	2.880	54744	137207	0.399
CN8-0-4-2	4.024	82929		0.604
CN8-0-4-3	2.430	79404		0.579

Table 15 - April 2012, 16 ft Test Results

Specimen ID	Strain Rate (in./in./sec)	Maximum Dynamic Load (lbf)	Average Maximum Static Load (lbf)	Dynamic/Static Load
TF16-400-4-1	0.735	35715	33101	1.079
TF16-400-4-2	0.840	47664		1.440
TF16-400-4-3	0.639	33964		1.026
CF16-400-4-1	2.792	54394	93957	0.579
CF16-400-4-2	4.250	50369		0.536
CF16-400-4-3	4.012	52201		0.556
TN16-400-4-1	0.400	20896	19929	1.049
TN16-400-4-2	0.331	22187		1.113
TN16-400-4-3	1.172	63753		3.199
TN16-400-4-4	0.500	32222		1.617
TN16-400-4-5	1.117	57333		2.877
TN16-0-4-1	0.951	63837	26168	2.440
TN16-0-4-2	0.744	38653		1.477
TN16-0-4-3	1.102	69992		2.675
CN16-400-4-1	4.865	50390	99338	0.507
CN16-400-4-2	3.495	59244		0.596
CN16-400-4-3	2.184	46375		0.467
CN16-400-4-4	2.147	53176		0.535
CN16-400-4-5	2.794	63759		0.642
CN16-0-4-1	12.103	153630	137207	1.120
CN16-0-4-2	6.254	114367		0.834
CN16-0-4-3	8.429	137804		1.004
CN16-cooled-4-1	4.006	87321	109885	0.795
CN16-cooled-4-2	4.843	109316		0.995
CN16-cooled-4-3	4.794	98173		0.893

Concrete Composition at Room Temperature

For compression tests with a drop height of 8 ft, the average DIF and strain rate were higher for FRC specimens than NWC specimens. The average DIF increased by 50% from 0.4 for CN8 to 0.6 for CF8 specimens. The average strain rate increased by 90% from 2.0 in./in./sec to 3.8 in./in./sec. This increase may in part be due to the increased drop weight from 92 lbf for NWC specimens to 158 lbf for FRC specimens.

The change in drop hammer weight was less extensive for compression tests with a drop height of 16 ft. A drop weight of 70.5 lbf was used for CN16 and a drop weight of 92 lbf was used for CF16. The CN16 specimens had an average DIF of 0.6 which increased by 33% to 0.8 for CF16 specimens. The average strain rates also increased from 4.7 in./in./sec to 6.9 in./in./sec, an increase of 45%. With similar drop weights, the FRC still had higher DIFs and strain rates when compared to NWC.

For the tensions tests with a drop height of 8 ft, comparable drop weights were used. The TN8 and TF8 specimens had respective drop weight of 70.5 lbf and 92 lbf. The TN8 specimens had an average DIF of 2.4 which decreased by 13% to 2.1 for TN16 specimens. However, the average strain rate increased by 40% from 0.8 to 1.1.

The same drop weight (49.5 lbf) was used for the TN16 and TF16 specimens. The TN16 specimens had an average DIF of 3.4 which decreased by 35% to 2.2 for TF16 specimens. The strain rate also decreased from 1.3 to 1.1, a decrease of 15%.

Overall, for both 8 ft and 16 ft drop height compression tests the average DIF and average strain rates increased when FRC was used in place of NWC. For tension tests the average DIF and average strain rates decreased when FRC was used in place of NWC. The strain rate did increase for the TF8 specimens, but decreased for TF16 specimens when compared to their corresponding NWC tests.

Concrete Composition at Elevated Temperature

For elevated temperature compression tests an 8 ft drop height with a 223 lbf drop weight was used. The average DIF decreased by 29% from 0.7 for CN8-400 to 0.5 for CF8-400. The average strain rate also decreased by 32% from 4.1 in./in./sec to 2.8 in./in./sec. For elevated compression tests with a 16 ft drop height a 136 lbf drop weight was used. Both CN16-400 and CF16-400 specimens had an average DIF of 0.6. The average strain rate increased by 19% from 3.1 for CN16-400 to 3.7 for CF16-400 specimens. Overall, at a drop height of 8 ft and a drop weight of 223 lbf, FRC specimens had a lower average DIF and strain rate, whereas at a drop height of 16 ft and a drop weight of 136 lbf, FRC performed similar to NWC.

For elevated temperature tension tests an 8 ft drop height with a 92 lbf drop weight was used. The average DIF decreased by 47% from 1.7 for TN8-400 to 0.9 for TF8-400. Both of these specimens had an average strain rate of 0.5 in./in./sec. For elevated temperature tension tests with a 16 ft drop height a 53.5 lbf drop weight was used. The average DIF decreased by 40% from 2.0 for TN16-400 to 1.2 for TF16-400. Both of these specimens had an average strain rate of 0.7 in./in./sec. At 400°F, for both 8 ft and 16 ft tests, the FRC specimens tested in tension had lower average DIFs than NWC, however, the average strain rate remained the same.

Temperature Effects for Normal Weight Concrete

For elevated temperature NWC compression tests at 8 ft drop heights a 223 lbf drop weight was used. Heating the specimens increased the DIF by 40% from 0.5 for CN8-R to 0.7 for CN8-400. The average strain rate also increased from 3.1 to 4.0, an increase of 32%. For elevated temperature, NWC compression tests with a 16 ft drop height a 136 lbf drop weight was used. Heating the specimen reduced the average DIF from 1.0 for CN16-R to 0.6 for CN16-400, a decrease of 40%. The average strain rate also decreased from 9.0 to 3.1, a decrease of 66%. For NWC compression tests at 400°F the DIF and strain rate increased for the 8 ft drop height, but decreased for the 16 ft drop height when compared with the room temperature tests.

For elevated temperature NWC tension tests at 8 ft drop heights a 92 lbf drop weight was used. Heating the specimens increased the DIF by 21% from 1.4 for TN8-R to 1.7 for TN8-400. The average strain rate, however, decreased from 0.6 to 0.5, a decrease of 17%. For NWC tension tests at 16 ft drop heights a 53.5 lbf drop weight was used. Heating these specimens decreased the averages DIF by 9% from 2.2 for TN16-R to 2.0 for TN16-400. The strain rate also decreased from 0.9 in./in./sec to 0.7 in./in./sec, a decrease of 22%. For NWC tension tests at 400°F the DIF increased for the 8 ft drop height, but the strain rate decreased when compared to room temperature tests. For the 16 ft drop height, both the DIF and strain rate decreased when the temperature was elevated.

A few additional compression tests with a drop height of 16 ft and a 136 lbf drop weight were performed on NWC specimens that were allowed to cool. The average DIF for these CN16-cooled specimens was 0.9 with an average strain rate of 4.5 in./in./sec. The CN16-400 had an average DIF of 0.6 with an average strain of 3.1 in./in./sec and the CN16-R specimens had an average DIF of 1.0 with an average strain rate of 9.0 in./in./sec. Allowing the concrete to cool increased the DIF and strain rate when compared to the heated specimens, but still did not perform as well as the room temperature specimens.

Temperature Effects for Fiber Reinforced Concrete

For elevated temperature FRC tests comparisons are made between July 2011 and April 2012 tests since no room temperature tests were done on FRC specimens in April 2012. Drop weights of 158 lbf and 223 lbf were used for CF8-R and CF8-400 specimens respectively. The average DIF decreased by 17% from 0.6 for CF8-R to 0.5 for CF8-400. The strain rate also decreased from 3.8 to 2.8 in./in./sec., a decrease of 26%. Drop weights of 92 lbf and 136 lbf were used for CF16-R and CF16-400 specimens respectively. The average DIF decreased by 25% from 0.8 for CF16-R to 0.6 for CF16-400. The strain rate also decreased from 6.8 to 3.7 in./in./sec, a decrease of 46%. Increasing the temperature for FRC compression tests decreased the DIF and strain rate for both 8 ft and 16 ft drop heights.

For elevated temperature FRC tension tests, similar drop weights were used in July 2011 and April 2012. A drop weight of 92 lbf was used for both TF8-R and TF8-400. The average DIF decreased from 2.1 for TN8-R to 0.9 for TF8-400, a decrease of 57%. The average strain rate also decreased from 1.1 to 0.5 in./in./sec, a decrease of 55%. Drop weights of 49.5 lbf and 53.5 lbf were used for TF16-R and TF16-400 specimens respectively. The average DIF decreased by 45% from 2.2 for TF16-R to 1.2 for TF16-400. The strain rate also decreased from 1.1 to 0.7 in./in./sec, a decrease of 36%. For FRC tension tests at elevated temperatures the DIF and strain

decreased for both 8 ft and 16 ft drop heights when compared with corresponding room temperature test results.

Conclusions

To determine how concrete is affected by dynamic loads, 4 in. diameter by 8 in. high cylinders were tested with various concrete materials, loading types and drop heights. Dynamic impact factors and strain rates were calculated to compare the results of these tests. The dynamic impact factor was simply computed by taking a ratio of maximum dynamic load to the corresponding average maximum static load. To determine the appropriate strain rate three methods were explored: the high speed camera method, the load cell method and the strain gauge method. The high speed camera method and load cell method gave strain rates that were higher than the load cell method. These two methods are representative of a local strain rate, whereas the load cell method provides a more global result. To compare different specimen types, the load cell method was used to determine the strain rates.

Various drop weights were used among the specimen types. The results of the same test types performed with differing drop weights were analyzed to determine if appropriate comparisons could be made. Although a difference was seen in the resulting DIF and strain rates, there was no distinct correlation between the drop weight and DIF or strain rate. Therefore, comparisons between tests with different drop weight have been carried out. The change in drop weight did have a greater effect on the strain rate than the DIF.

The dynamic tests were reviewed by comparing the effects of drop height for each specimen type and room and elevated temperatures. For NWC, increasing the drop height from 8 ft to 16 ft increased the resulting DIF and strain rate for both compression and tension. For FRC tension specimens, increasing the drop height had little effect. However, the FRC compression specimens saw an increase in DIF and strain rate with the increased drop height.

When the drop height was increased for elevated temperature specimens, the DIF and strain rate of NWC in tension increased, whereas, compression tests saw a decrease. For FRC specimens tested at elevated temperatures, an increase in drop height increased the DIF and strain rate for both compression and tension tests.

For compression tests at room temperature and with drop heights of both 8 ft and 16 ft, FRC specimens had higher DIFs and strain rates than NWC. When tested in tension, FRC specimens had a lower DIF and lower strain rate than NWC for the 8 ft drop height. The 16 ft drop height also had a lower DIF for but saw an increase in strain rate.

For compression tests at elevated temperatures, FRC specimens with 8 ft drop heights had lower DIFs and strain rates. When tested with a 16 ft drop height, FRC and NWC specimens performed similarly. For the tension tests at elevated temperatures, FRC specimen had lower DIFs and strain rates than NWC for both the 8 ft and 16 ft drop heights.

For NWC compression tests, elevating the temperature of the concrete resulted in an increased DIF and strain rate for the 8 ft drop height, but a decrease for the 16 ft drop height. For tension

tests the DIF increased and the strain rates decreased for the 8 ft drop height specimens. The 16 ft drop height specimens saw a reduction in DIF and strain rate when heated. For FRC compression tests at elevated temperatures, the DIF and strain rate decreased for both compression and static tests with both 8 ft and 16 ft drop heights.

From the few cooled NWC specimens that were tested in compression at 16 ft drop height, it was found that the DIF increased from when compared to the heated concrete, but was not as high as the room temperature concrete. Additional testing may be performed to further analyze the effects of cooling on concrete specimens with both NWC and FRC. It may be of interest to also investigate the size of the specimens and the effect this has on the results.

References

1. Garfield, T.T. (2011), "Performance of Reinforced Concrete Panels During Blast Loading," Master of Science Thesis, University of Utah, Salt Lake City, Utah.
2. PCB Piezotronic Inc. Force/Torque Division "Model 206C ICP® Dynamic Force Sensor Installation and Operation Manual."
3. American Society for Testing Material (2004), "ASTM C496/C496 M-04e1 Standard Test Method for Splitting Tensile Strength of Cylindrical Concrete Specimens." ASTM International, West Conshohocken.
4. American Society for Testing Material (2012). "ASTM C39/C39M-10 Standard Test Method for Splitting Compressive Strength of Cylindrical Concrete Specimens." ASTM International, West Conshohocken, PA.
5. DIAdem (2009). DIAdem Version 11.1, National Instruments Corp., Austin, TX.
6. Phantom (2012). Phantom Cine Viewer Version 2.0, Phantom Vision Research. Retrieved from <http://www.visionresearch.com>.
7. Malvar, L.J. and Ross, C.A. (1998), "Review of Strain Rate Effects for Concrete in Tension." ACI Materials Journal, 95(6), 735-739.
8. Millard, S.G., Molyneaux T.C.K. and Barnett, S.J. (2010), "Dynamic Enhancement of Blast-resistant Ultra High Performance Fibre-reinforce Concrete under Flexural and Shear Loading." International Journal of Impact Engineering, 37, 405-413.

Appendix A

July 2011 - Photographs of Tested Specimens



Figure A.1 - TF Specimens after Static Tests



Figure A.2 - TN Specimens after Static Test



Figure A.3 - Specimen TF8-2 after Dynamic Test



Figure A.4 – Specimen CF8-2 after Dynamic Test



Figure A.5 - Specimen TN8-2 after Dynamic Test



Figure A.6 - Specimen CN8-2 after Dynamic Test



Figure A.7 - Specimen TF16-2 after Dynamic Test



Figure A.8 - Specimen CF16-2 after Dynamic Test



Figure A.9 - Specimen TN16-2 after Dynamic Test



Figure A.10 - Specimen CN16-2 after Dynamic Test

Appendix B

July 2011 - Load Data Graphs

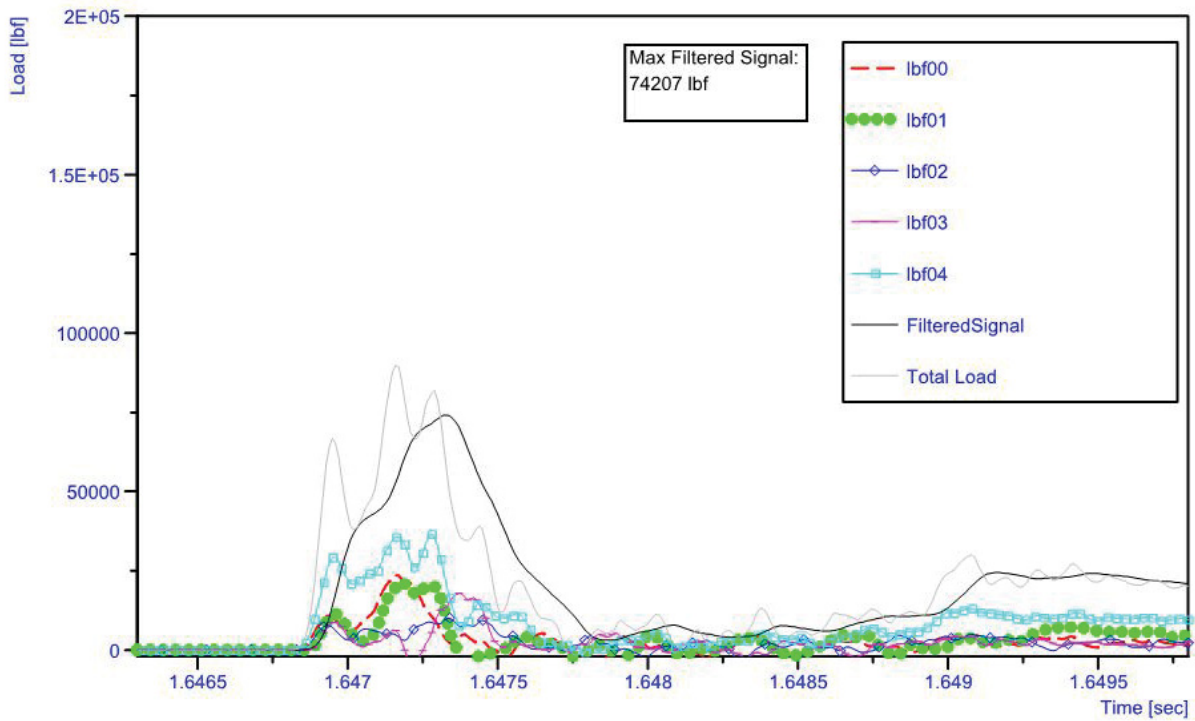


Figure B.1 – TF8-2 Load Data

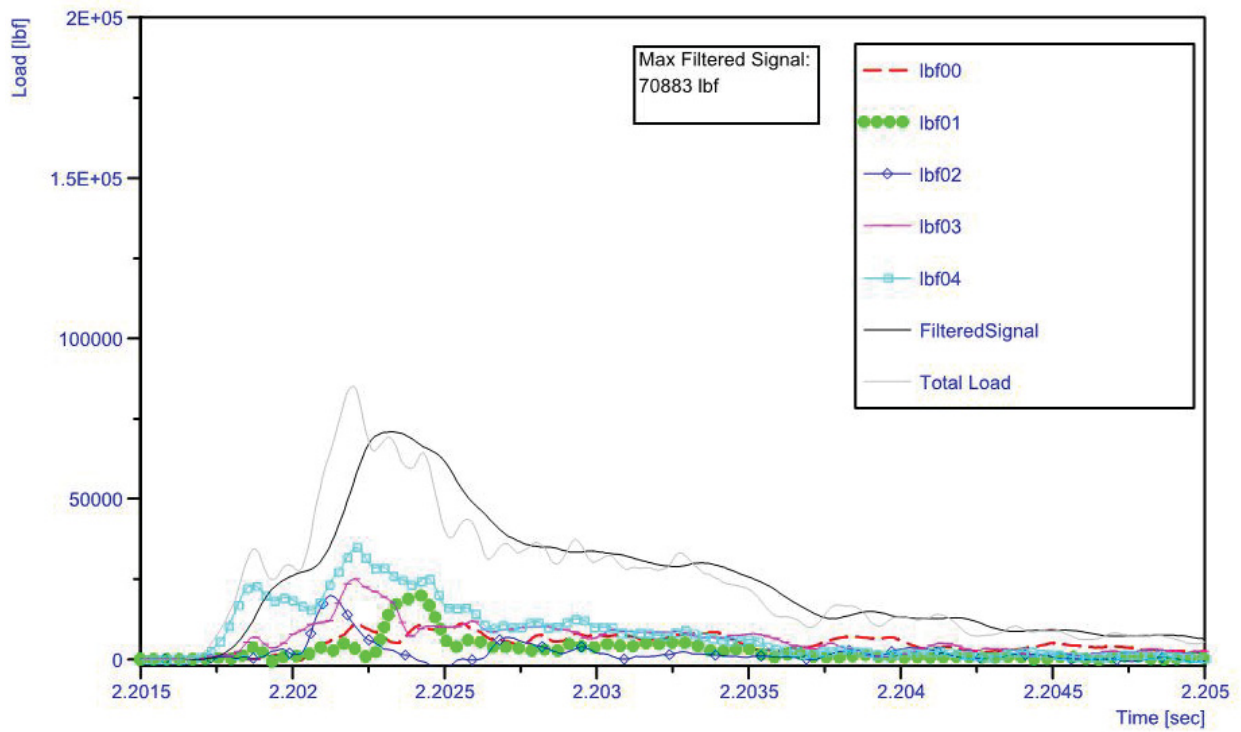


Figure B.2 - CF8-2 Load Data

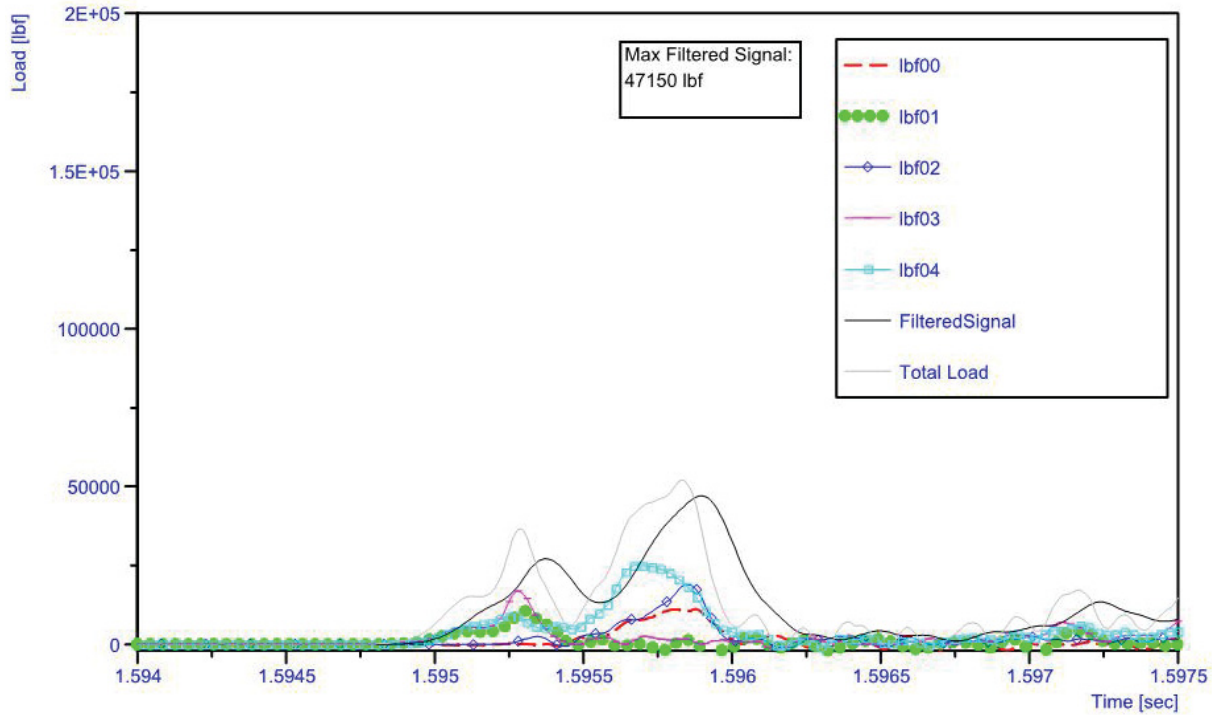


Figure B.3 - TN8-2 Load Data

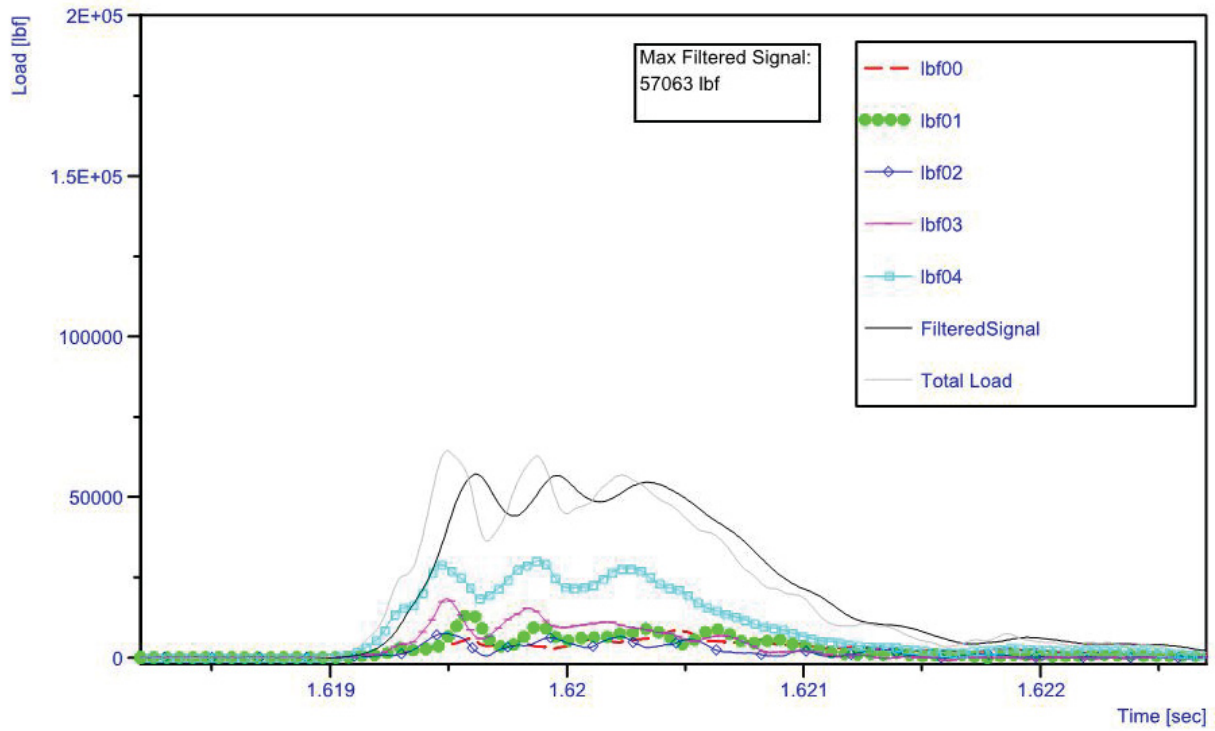


Figure B.4 - CN8-2 Load Data

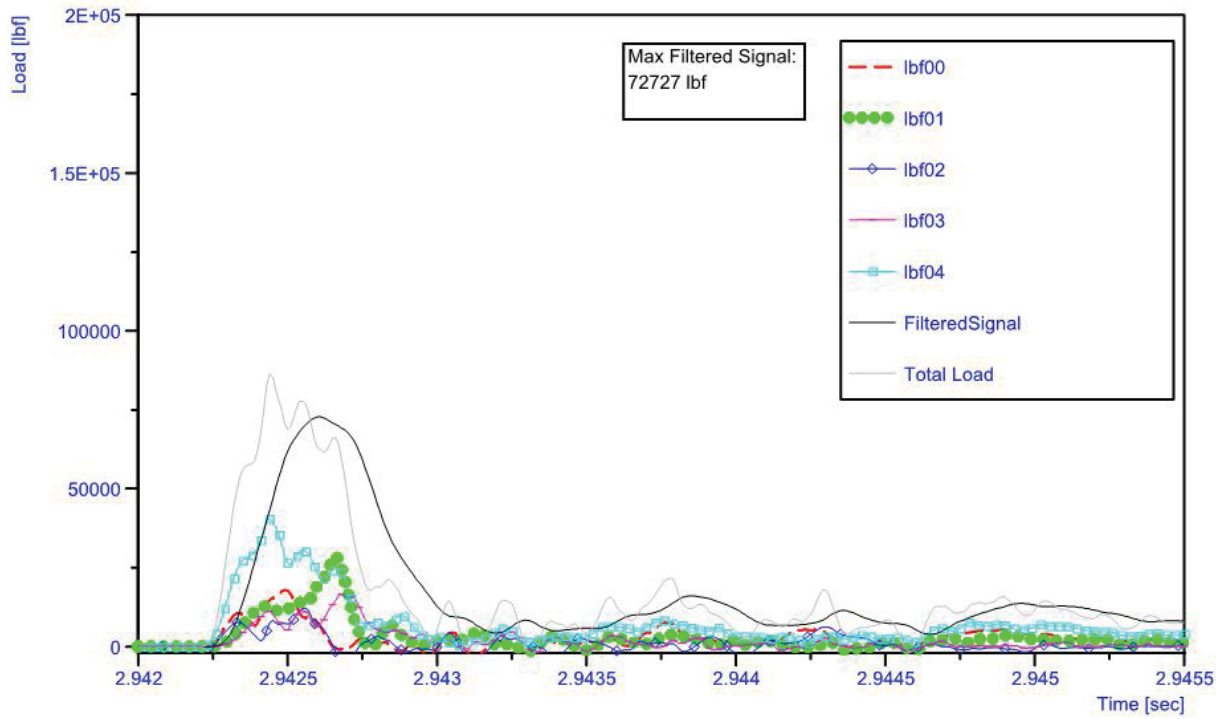


Figure B.5 - TF16-2 Load Data

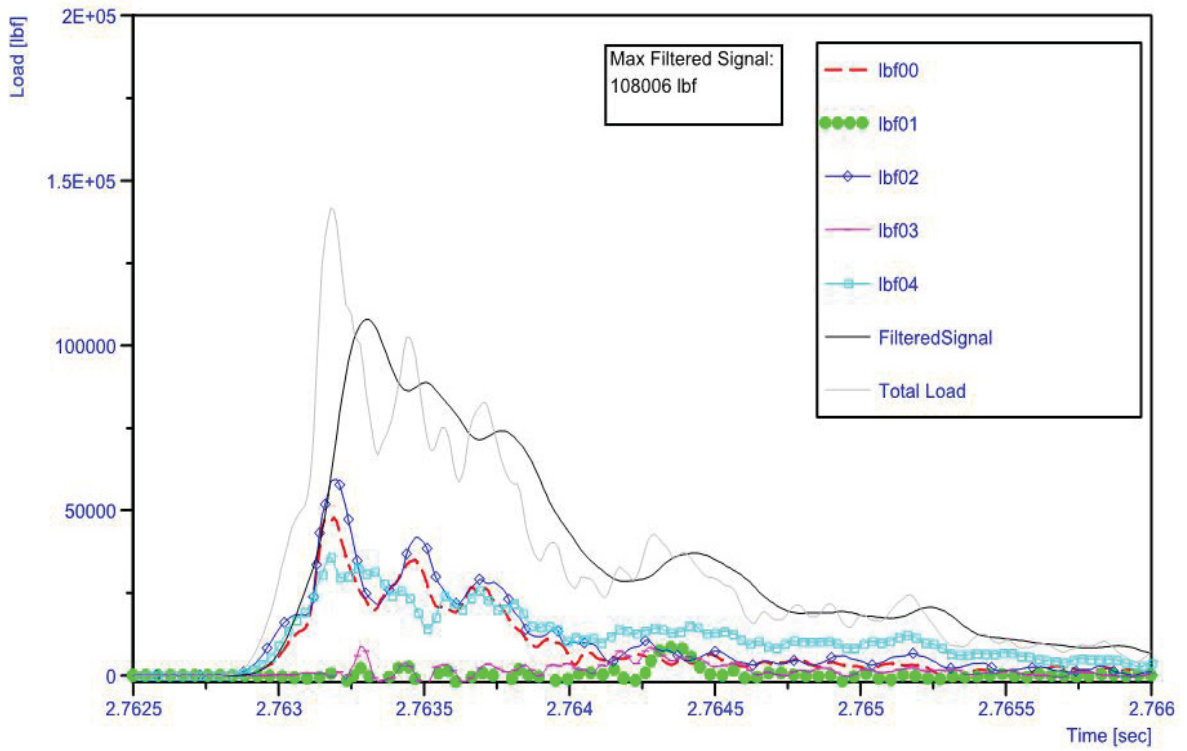


Figure B.6 - CF16-2 Load Data

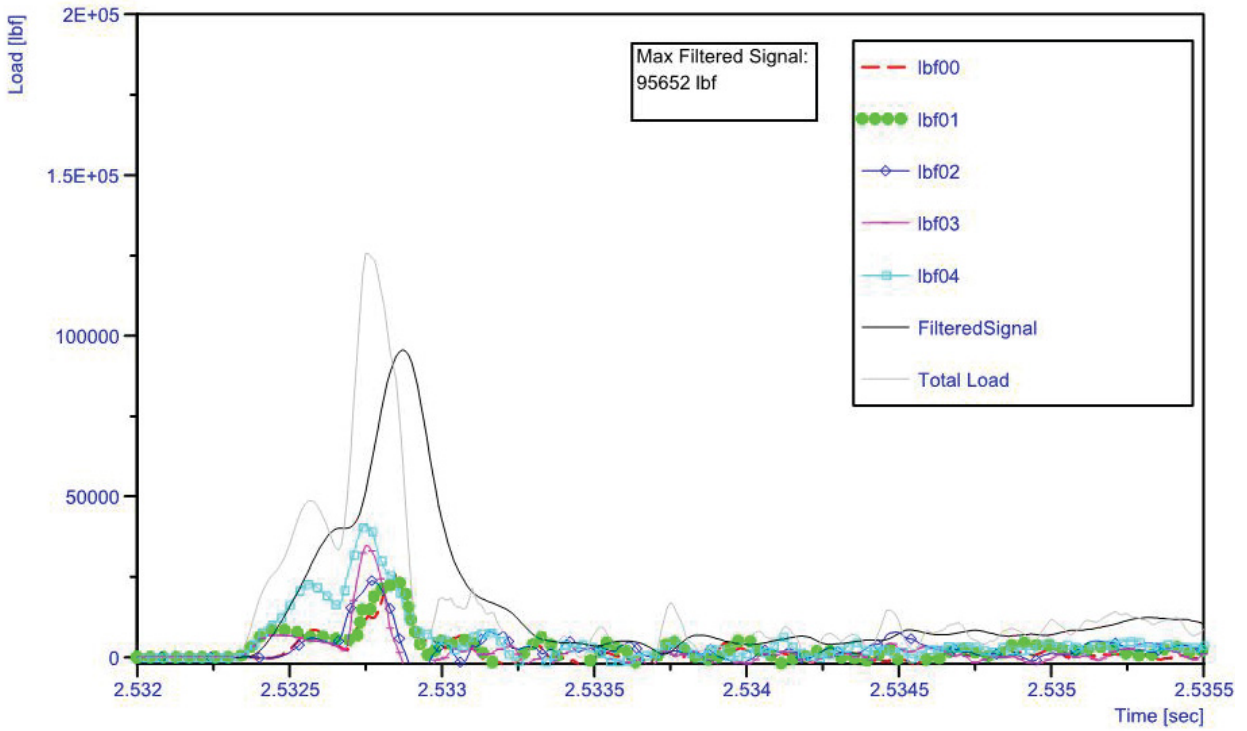


Figure B.7 - TN16-2 Load Data

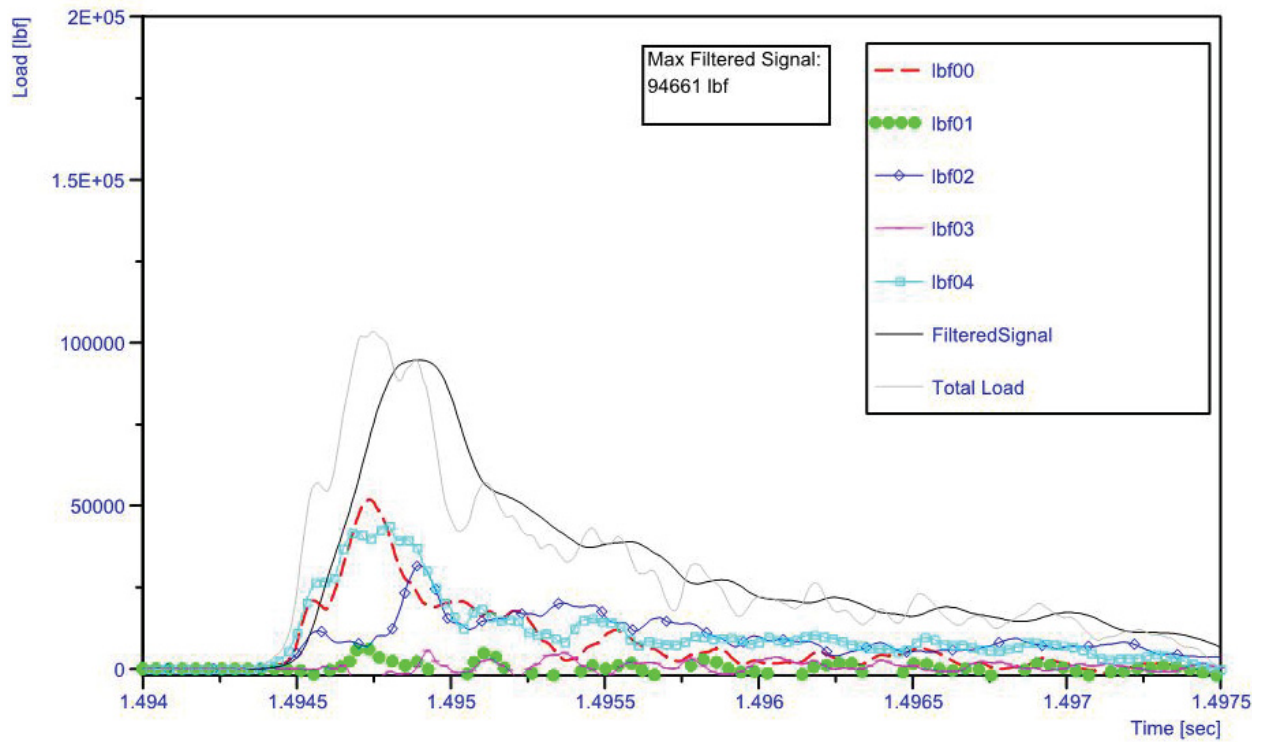


Figure B.8 - CN16-2 Load Data

Appendix C

July 2011 - Strain Data Graphs

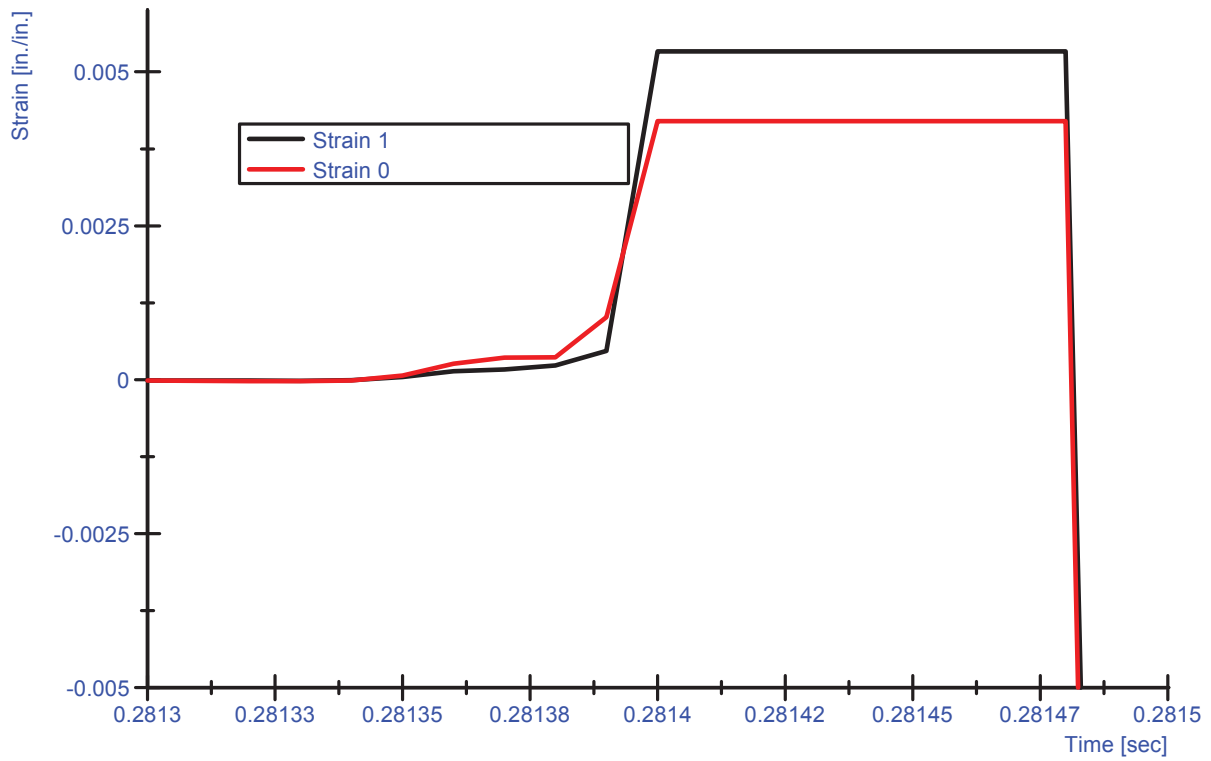


Figure C.1 – Specimen TN8-2 Strain Data for Dynamic Test

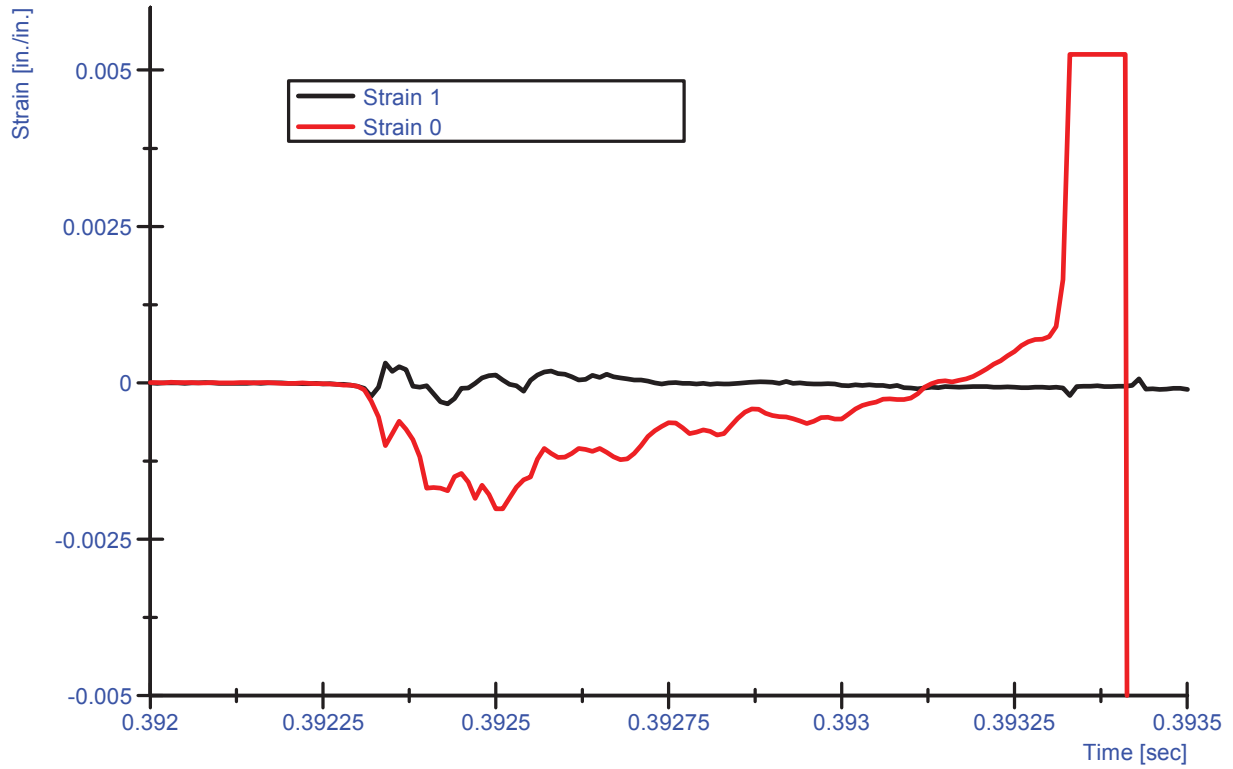


Figure C.2 – Specimen CF8-2 Strain Data for Dynamic Test

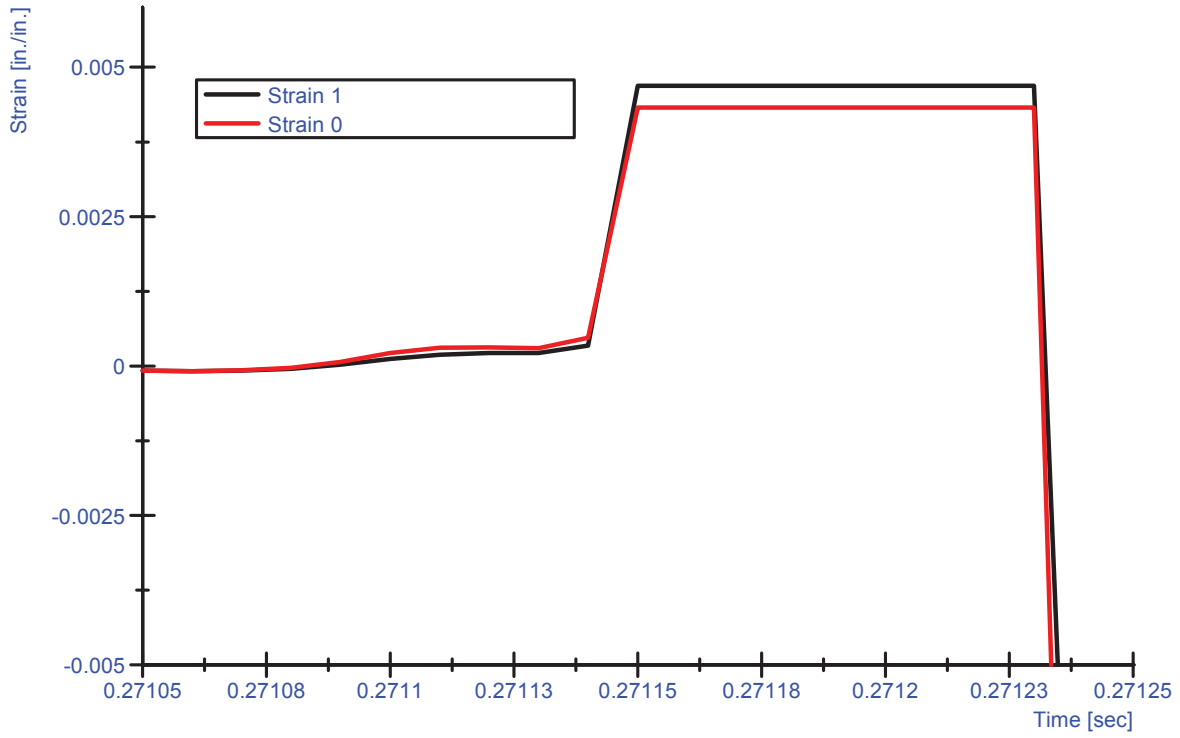


Figure C.3 – Specimen TN8-2 Strain Data for Dynamic Test

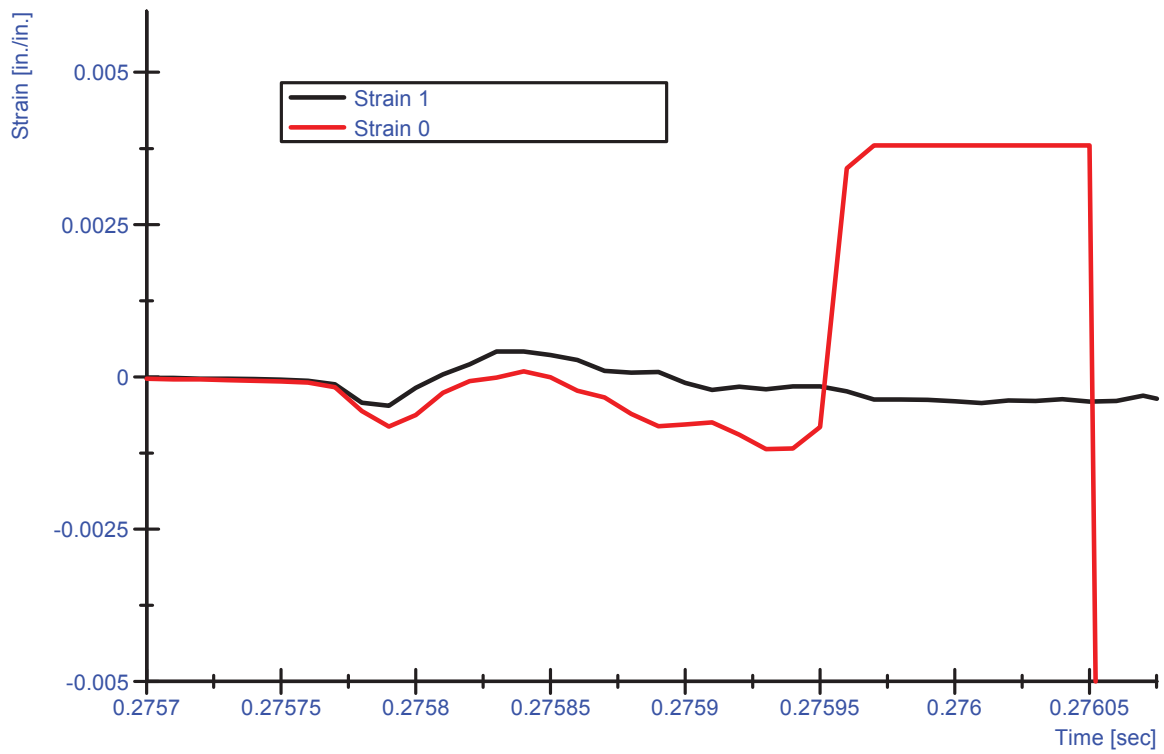


Figure C.4 – Specimen CN8-2 Strain Data for Dynamic Test

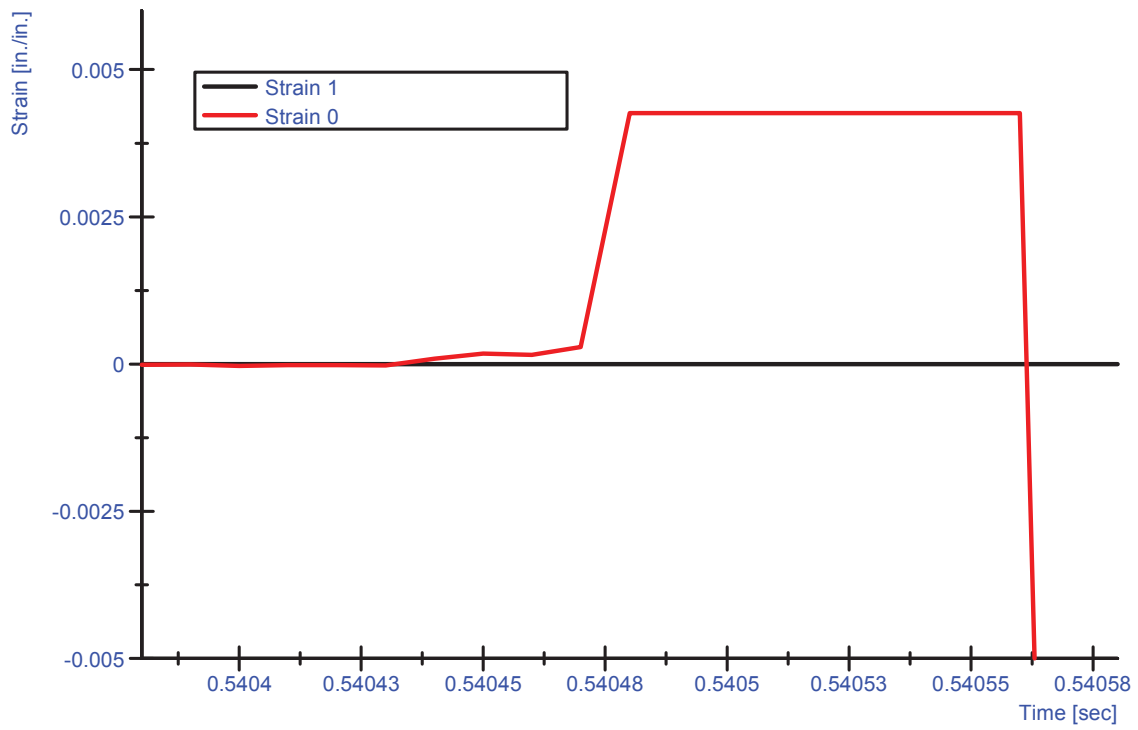


Figure C.5 – Specimen TF16-2 Strain Data for Dynamic Test

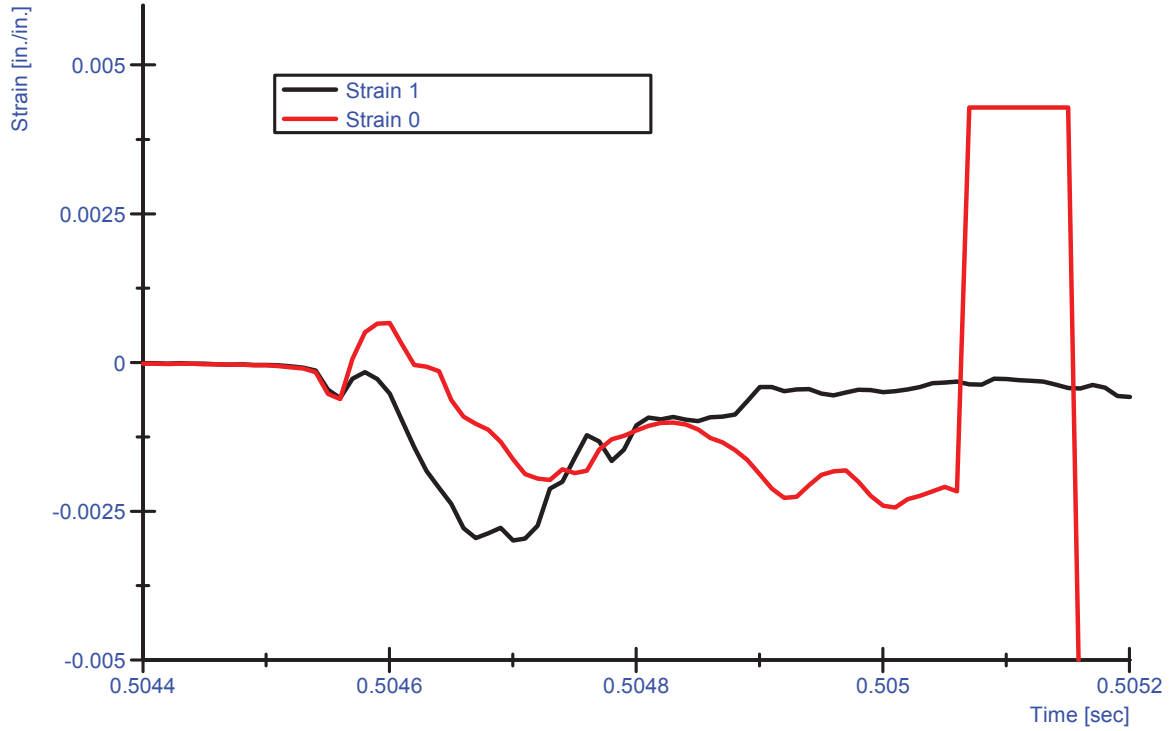


Figure C.6 – Specimen CF16-2 Strain Data for Dynamic Test

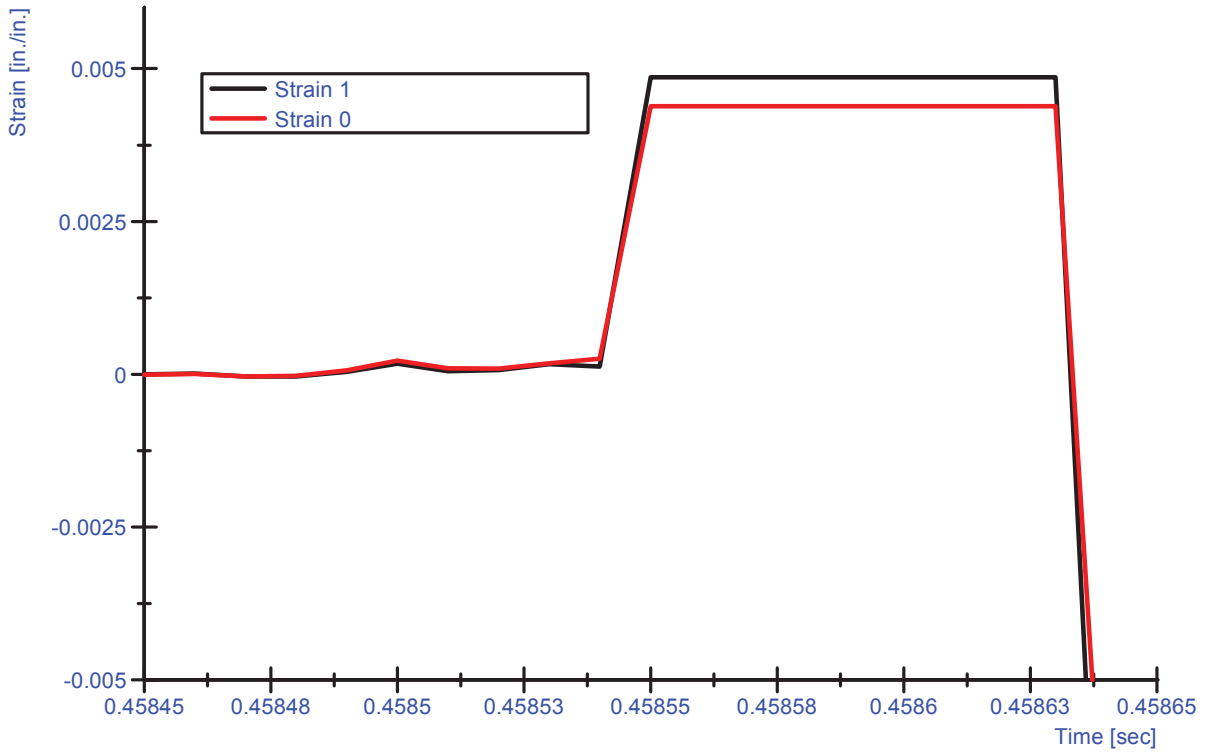


Figure C.7 – Specimen TN16-2 Strain Data for Dynamic Test

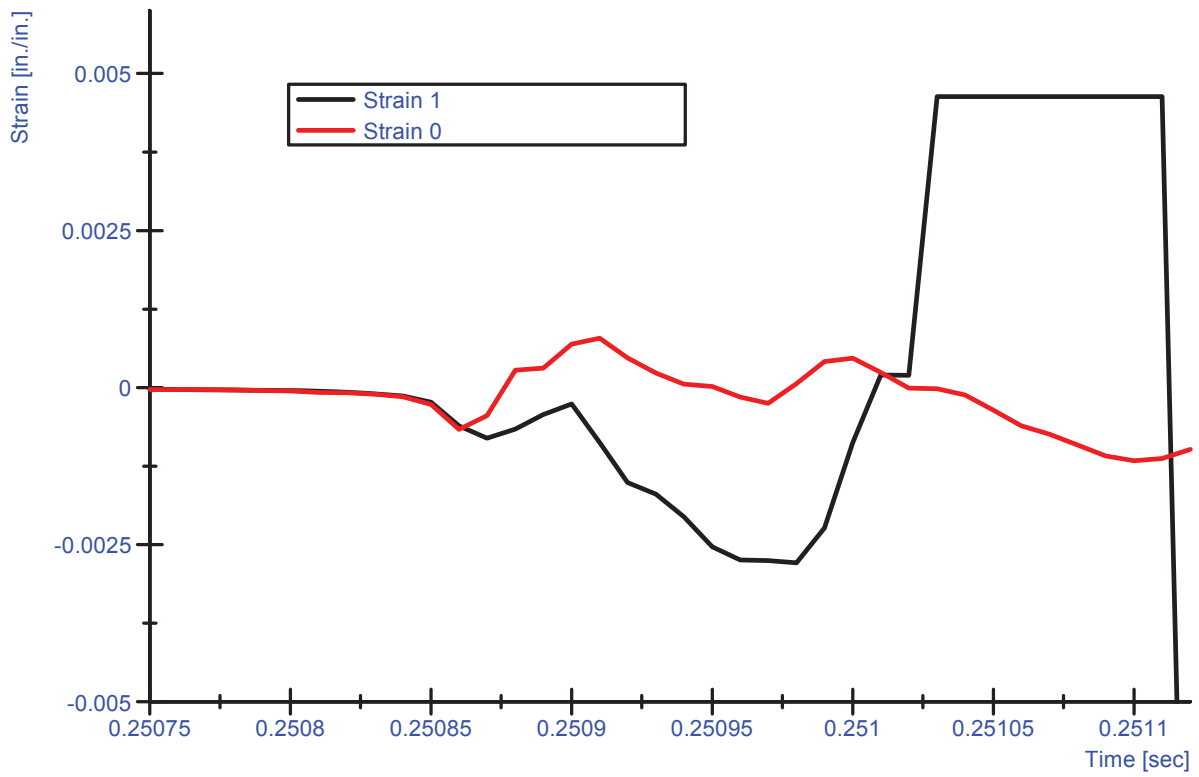


Figure C.8 – Specimen CN16-2 Strain Data for Dynamic Test

Appendix D

April 2012 - Photographs of Tested Specimens



Figure D.1 - CF0-0-4



Figure D.2 - CN0-0-4



Figure D.3 - TF0-400-4



Figure D.4 - CF0-400-4



Figure D.5 - TN0-400-4



Figure D.6 - CN0-400-4



Figure D.7 – Specimen TF8-400-4-1 after Dynamic Test



Figure D.8 – Specimen CF8-400-4-1 after Dynamic Test



Figure D.9 – Specimen TN8-400-4-1 after Dynamic Test



Figure D.10 - Specimen TN8-0-4-3 after Dynamic Test



Figure D.11 - Specimen CN8-400-4-4 after Dynamic Test



Figure D.12 - Specimen CN8-0-4-3 after Dynamic Test



Figure D.13 - Specimen TF16-400-4-1 after Dynamic Test



Figure D.14 – Specimen TF16-400-4-3 with Melted Fibers after Dynamic Test



Figure D.15 - Specimen CF16-400-4-1 after Dynamic Test



Figure D.16 – Specimen TN16-400-4-4 after Dynamic Test



Figure D.17 - Specimen TN16-0-4-1 after Dynamic Test



Figure D.18 – Specimen CN16-400-4-4 after Dynamic Test



Figure D.19 - Specimen CN16-0-4-1 after Dynamic Test



Figure D.20 - Specimen CN16-cooled-4-3

Appendix E

April 2012 - Load Graphs

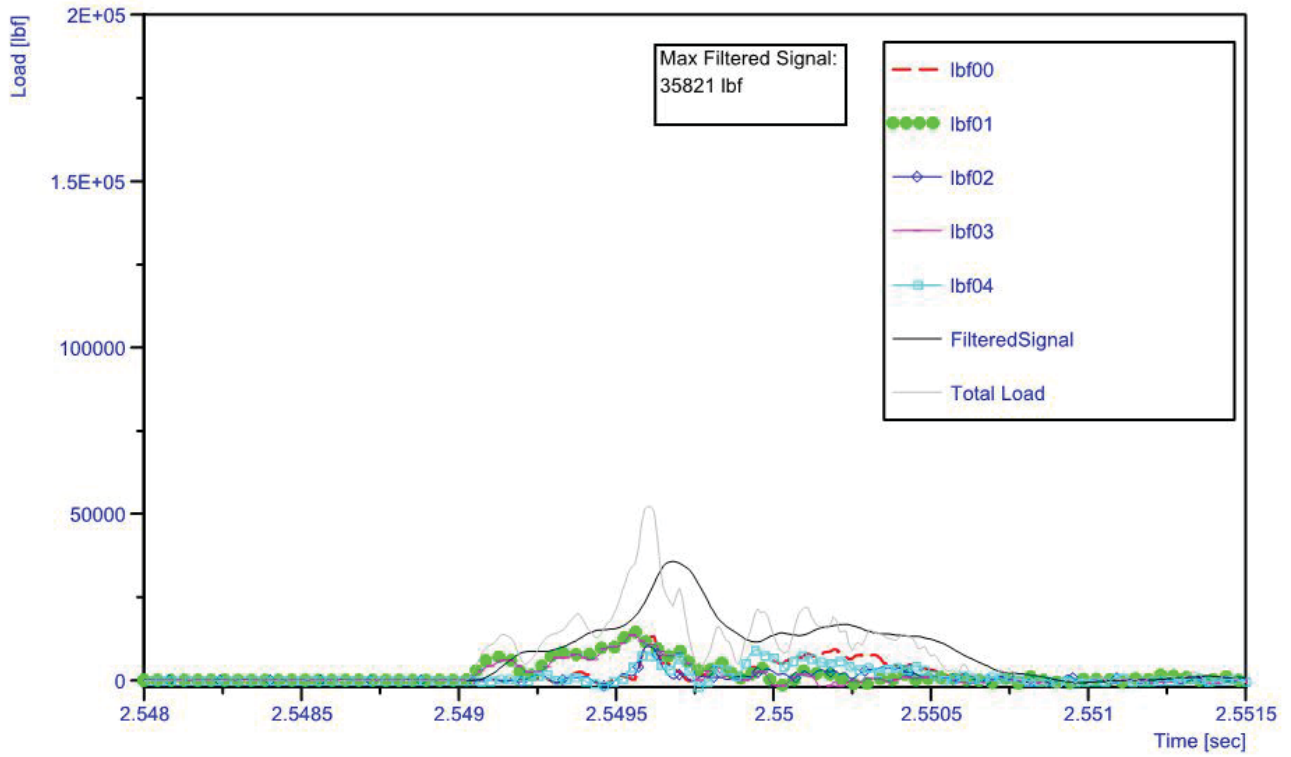


Figure 0.1 - TF8-400-4-1 Load Data

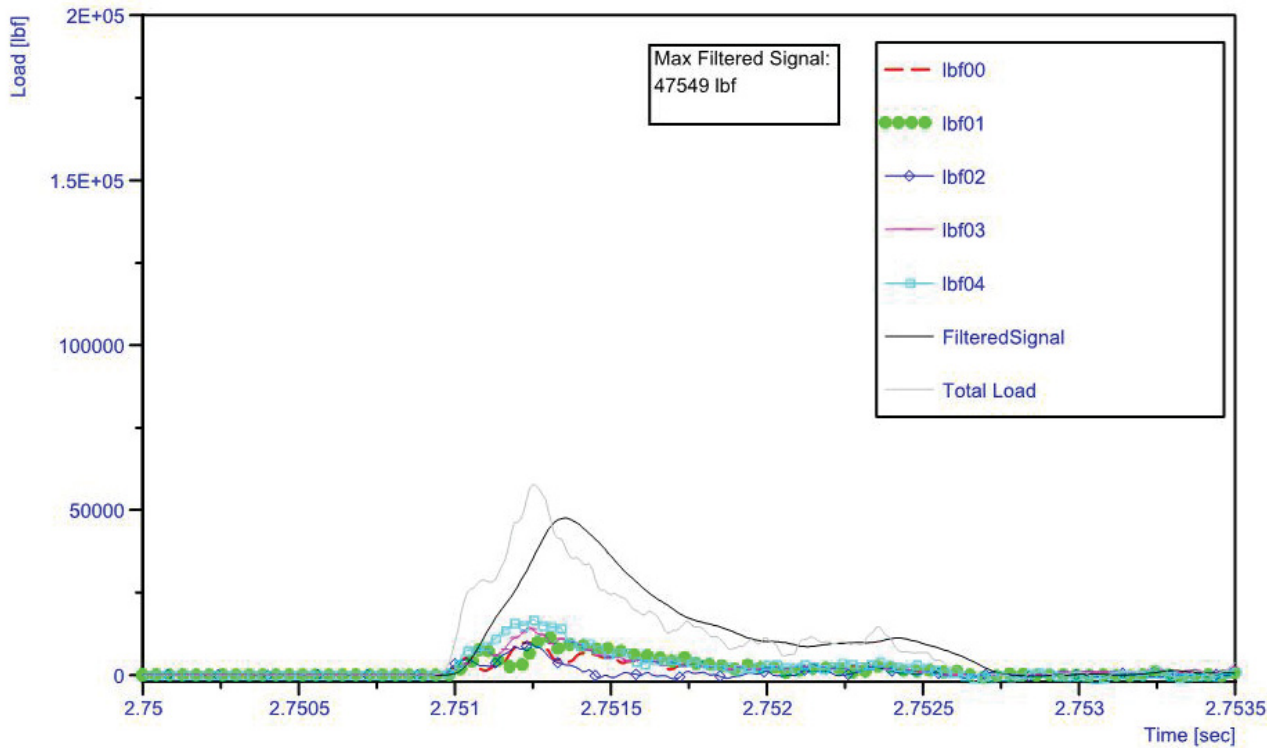


Figure 0.2 - CF8-400-4-1 Load Data

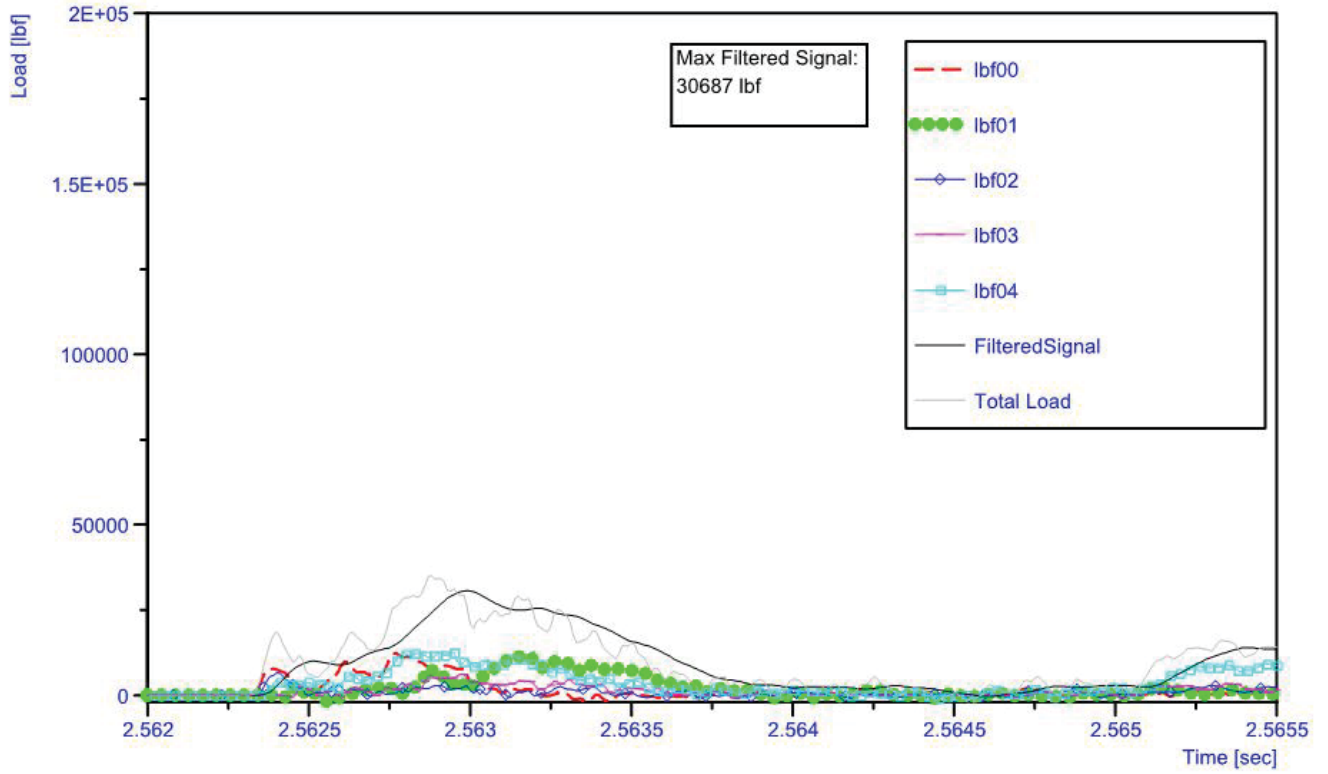


Figure 0.3 - TN8-400-4-1 Load Data

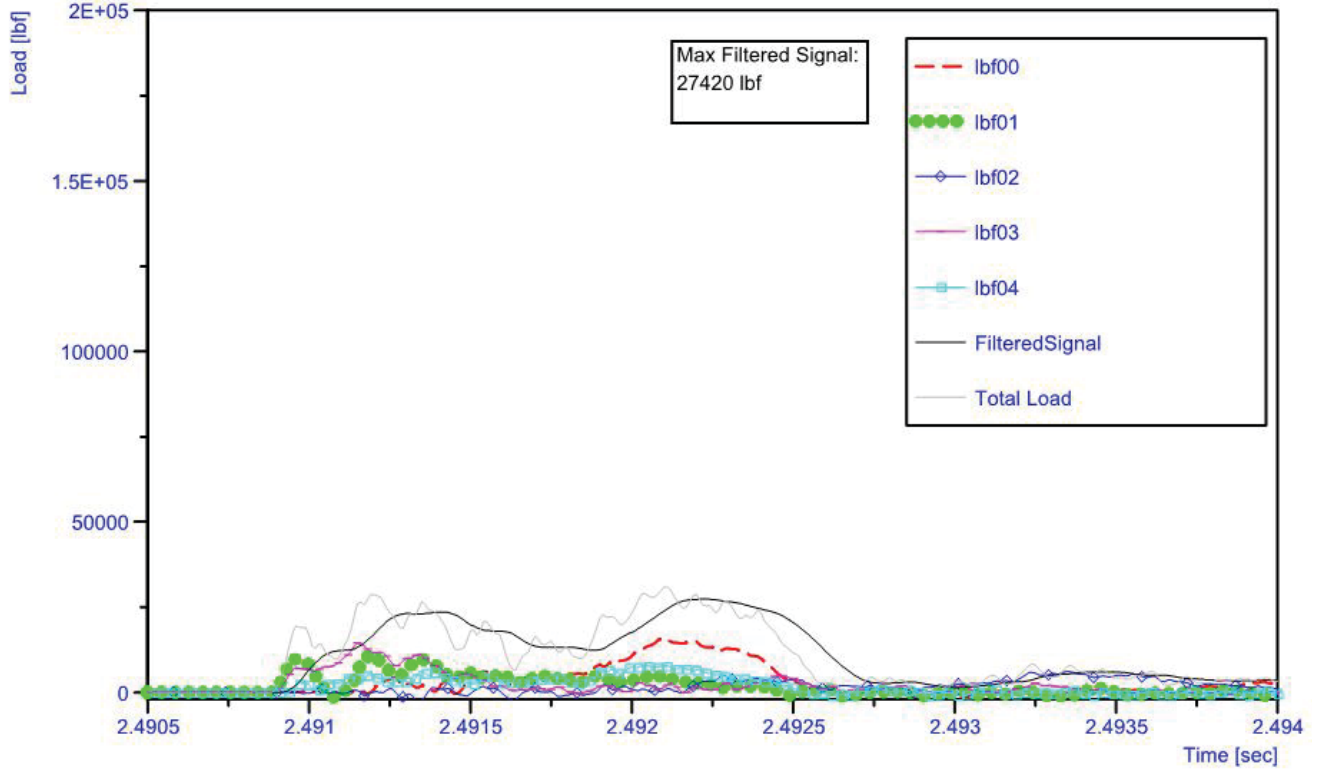


Figure 0.4 - TN8-0-4-3 Load Data

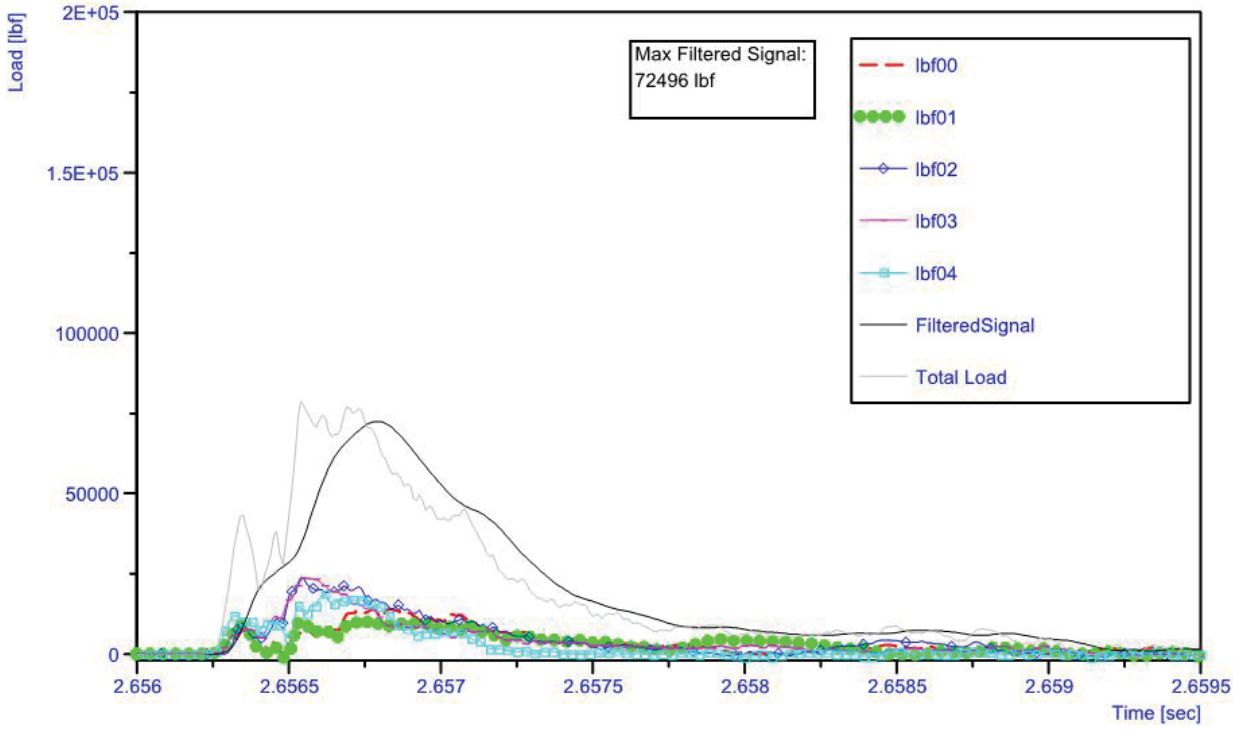


Figure 0.5 - CN8-400-4-4 Load Data

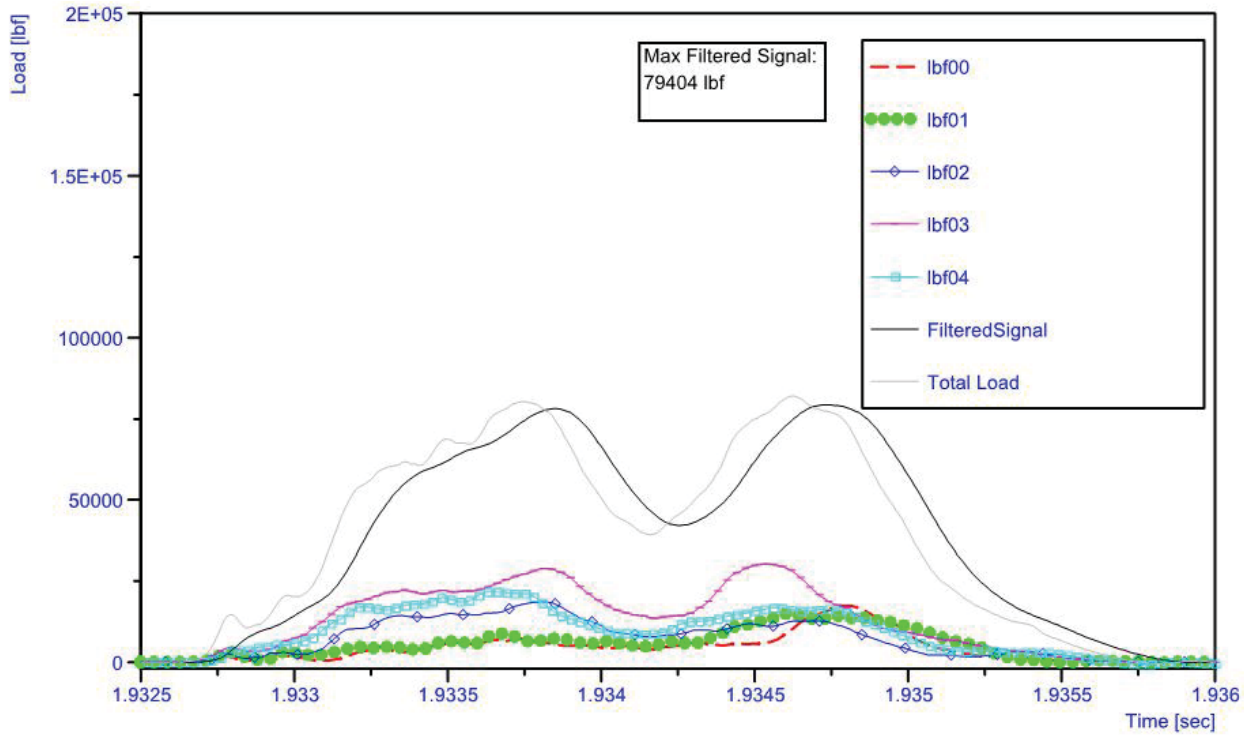


Figure 0.6 - CN8-0-4-3 Load Data

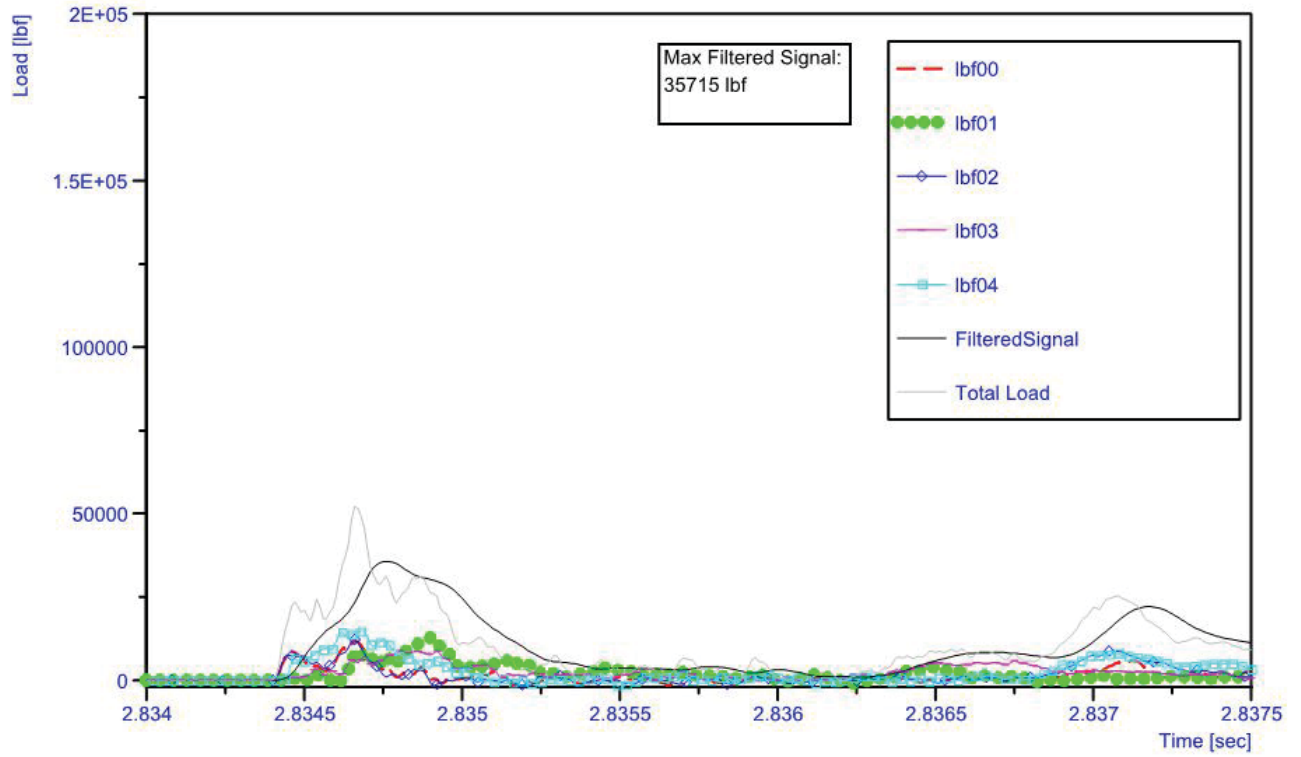


Figure 0.7 - TF16-400-4-1 Load Data

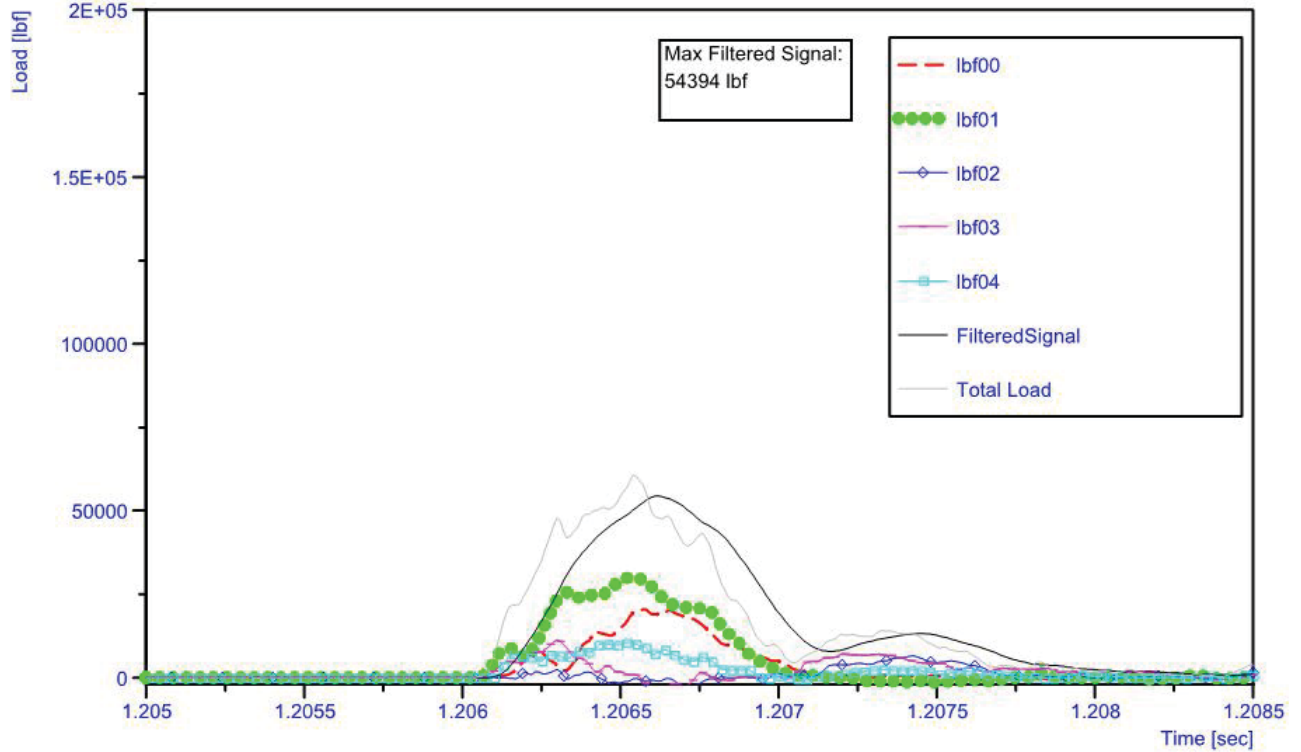


Figure 0.8 - CF16-400-4-1 Load Data

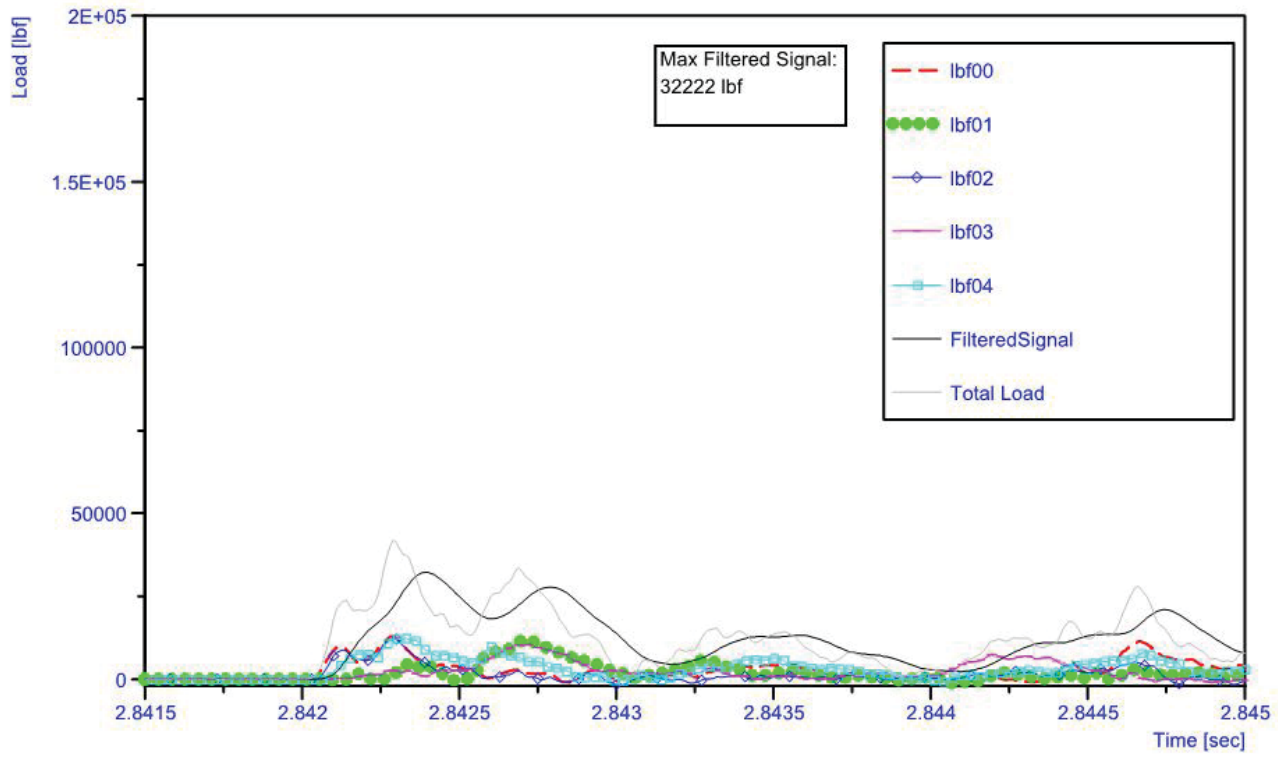


Figure 0.9 - TN16-400-4-4 Load Data

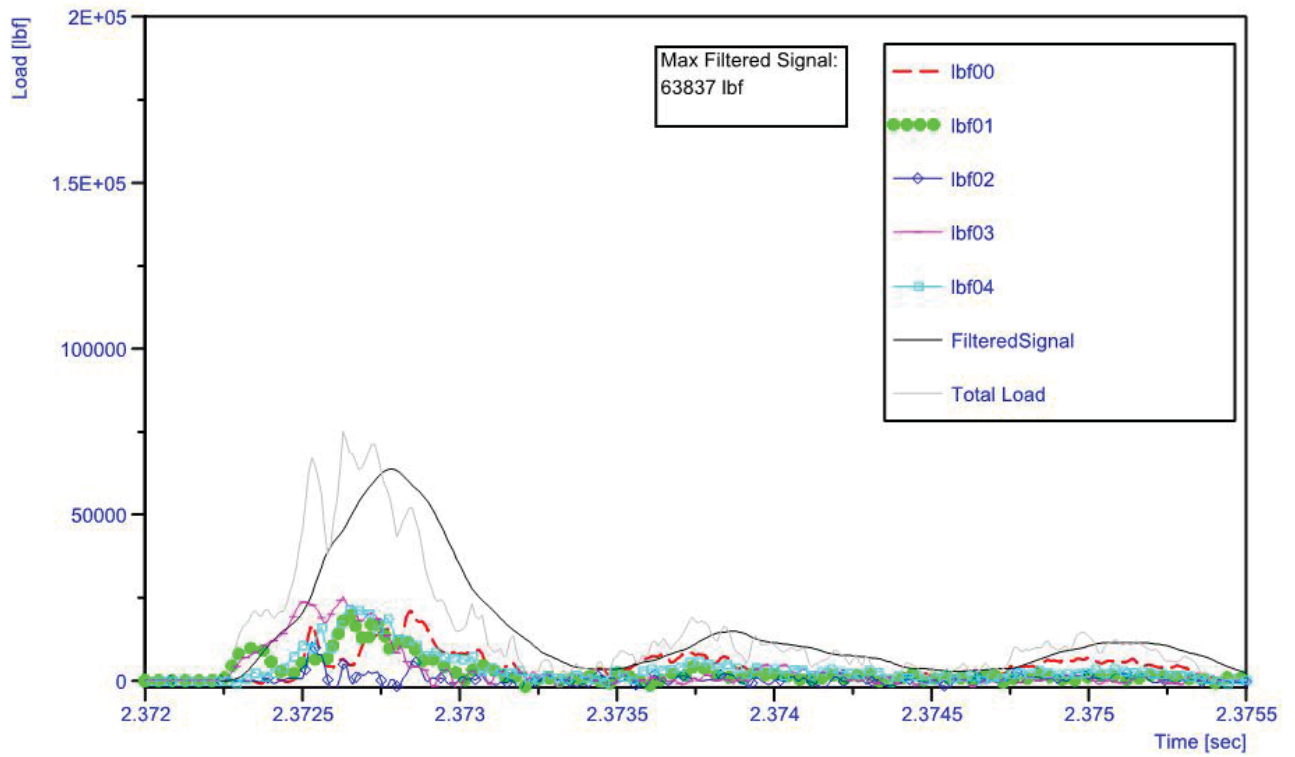


Figure 0.10 - TN16-0-4-1 Load Data

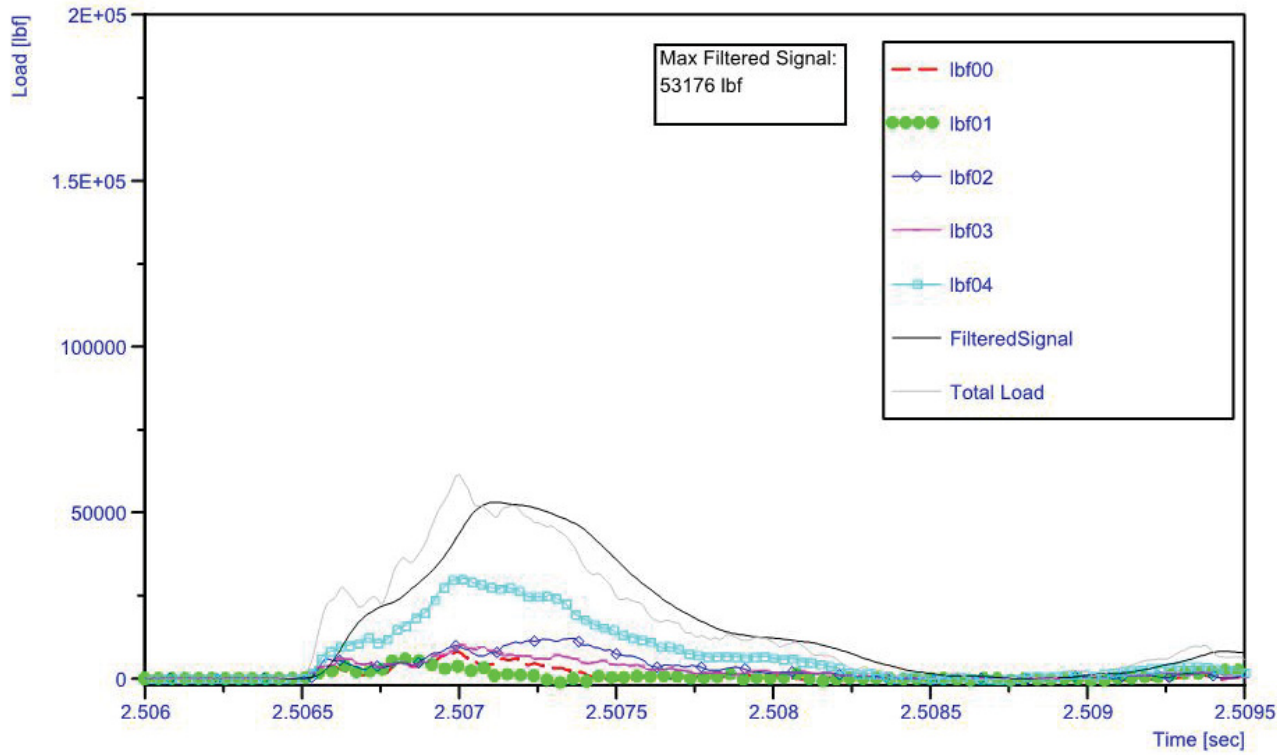


Figure 0.11 - CN16-400-4-4 Load Data

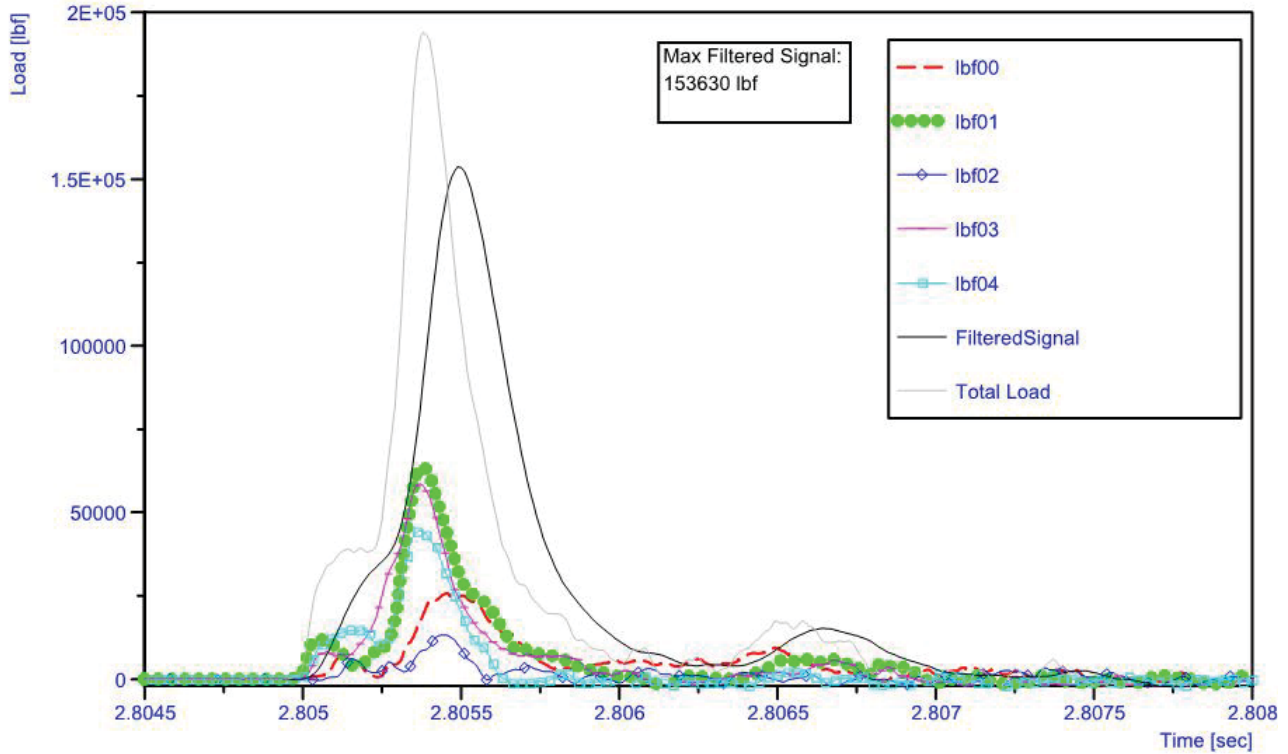


Figure 0.12 - CN16-0-4-1 Load Data

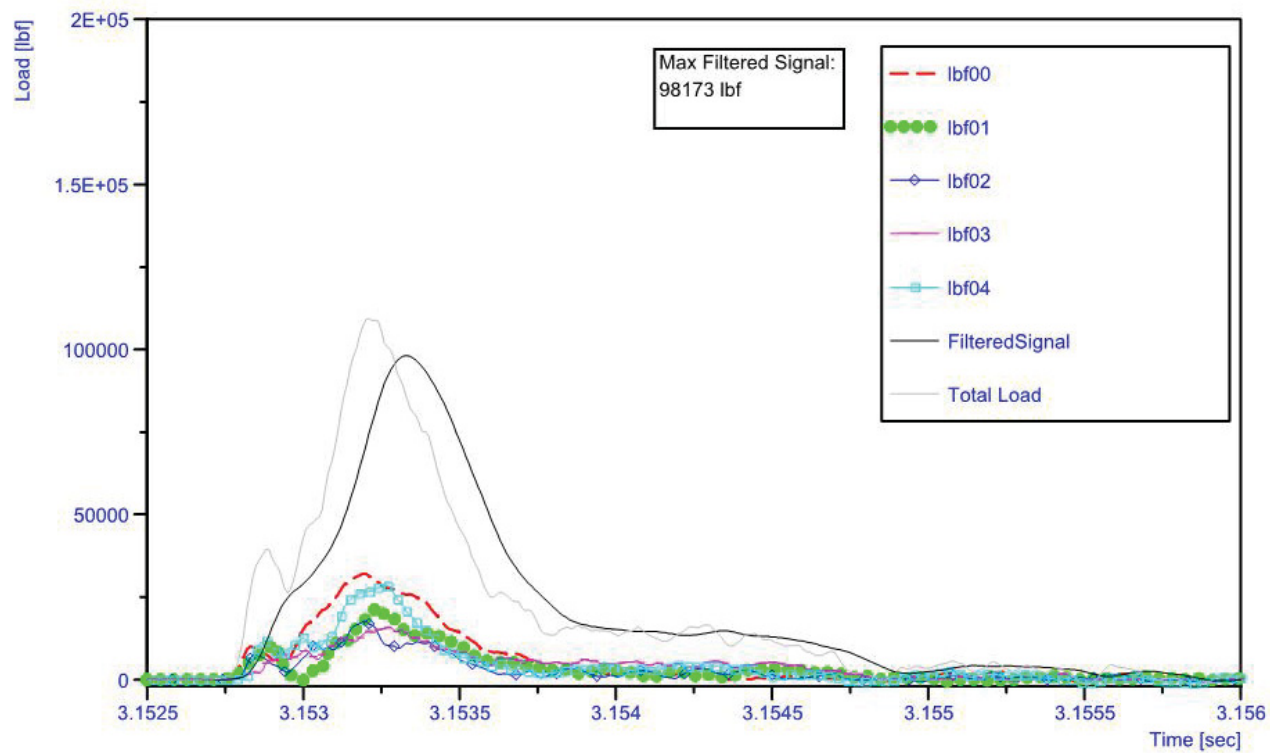


Figure 0.13 - CN16-cooled-4-3 Load Data